

# Thermodynamic, kinetic and solid-state study of divalent metal complexes of 1,4,8,11-tetraazacyclotetradecane (cyclam) bearing two *trans* (1,8-)methylphosphonic acid pendant arms†

Ivona Svobodová,<sup>a</sup> Přemysl Lubal,<sup>\*a</sup> Jan Plutnar,<sup>b</sup> Jana Havlíčková,<sup>b</sup> Jan Kotek,<sup>b</sup> Petr Hermann<sup>\*b</sup> and Ivan Lukeš<sup>b</sup>

Received 3rd March 2006, Accepted 14th September 2006

First published as an Advance Article on the web 22nd September 2006

DOI: 10.1039/b603251f

Divalent metal complexes of macrocyclic ligand 1,4,8,11-tetraazacyclotetradecane-1,8-bis(methylphosphonic acid) (1,8-H<sub>4</sub>te2p, H<sub>4</sub>L) were investigated in solution and in the solid state. The majority of transition-metal ions form thermodynamically very stable complexes as a consequence of high affinity for the nitrogen atoms of the ring. On the other hand, complexes with Mn<sup>2+</sup>, Pb<sup>2+</sup> and alkaline earth ions interacting mainly with phosphonate oxygen atoms are much weaker than those of transition-metal ions and are formed only at higher pH. The same tendency is seen in the solid state. Zinc(II) ion in the octahedral *trans*-O<sub>2</sub>O-[Zn(H<sub>2</sub>L)] complex is fully encapsulated within the macrocycle (N<sub>4</sub>O<sub>2</sub> coordination mode with protonated phosphonate oxygen atoms). The polymeric {[Pb(H<sub>2</sub>L)(H<sub>2</sub>O)<sub>2</sub>·6H<sub>2</sub>O]<sub>n</sub> complex has double-protonated secondary amino groups and the central atom is bound only to the phosphonate oxygen atoms. The phosphonate moieties bridge lead atoms creating a 3D-polymeric network. The [{(H<sub>2</sub>O)<sub>3</sub>Mn}<sub>2</sub>(μ-H<sub>2</sub>L)](H<sub>2</sub>L)·21H<sub>2</sub>O complex contains two pentaquamanganese(II) moieties bridged by a ligand molecule protonated on two nitrogen atoms. In the complex cation, oxygen atoms of the phosphonate groups on the opposite sites of the ring occupy one coordination site of each metal ion. The second ligand molecule is diprotonated and balances the positive charge of the complex cation. Complexation of zinc(II) and cadmium(II) by the ligand shows large differences in reactivity of differently protonated ligand species similarly to other cyclam-like complexes. Acid-assisted dissociations of metal(II) complexes occur predominantly through triprotonated species [M(H<sub>3</sub>L)]<sup>+</sup> and take place at pH < 5 (Zn<sup>2+</sup>) and pH < 6 (Cd<sup>2+</sup>).

## Introduction

Investigations of highly thermodynamically stable and kinetically inert complexes (often formed by macrocyclic ligands)<sup>1–5</sup> have been stimulated by their applications in several areas, such as the contrast agents (CA) in magnetic resonance imaging (MRI),<sup>6–9</sup> for labelling of biomolecules with metal radioisotopes for both diagnostic and therapeutic purposes<sup>10–14</sup> or for luminescence optical imaging utilizing some lanthanide(III) ions which may be used for determination of a physiological status of tissues (healthy/diseased, change in pH or concentration of ions or metabolites *etc.*).<sup>15,16</sup> In the above medicinal utilizations, the harmful metal ion or radioisotope must not be deposited anywhere in body and the complex must be eliminated off unchanged from body.

In radiotherapy or diagnosis utilizing radioisotopes several elements are widely used, nowadays mostly technetium, iodine and fluorine. However, metal radioisotopes offer some advantages as they exhibit a wide range of physical properties (type of emitted particles, particle energy). Some of such metal radioisotopes (*e.g.* isotopes of Ga, In, Y and lanthanides) are routinely used in medicine as some suitable ligands for them have been found.<sup>10–14</sup> However, there is still a high demand to find more convenient ligands for these and other metal radioisotopes. The other metal radioisotopes include also clinically used Cu isotopes<sup>17</sup> (mostly β-emitters) or less common Bi, Pb and Tl isotopes<sup>18</sup> (α-emitters) having a great therapeutical potential but with almost no available suitable ligands. Such investigations are a living field of modern coordination chemistry.

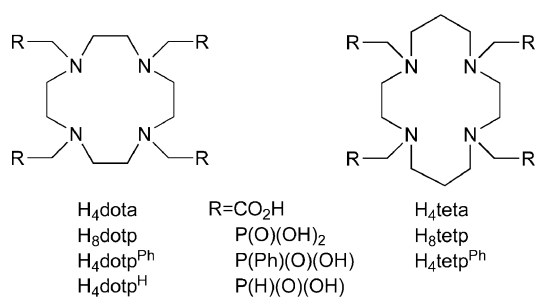
As mentioned above, these metal complexes may be useful in medicine (in MRI and nuclear medicine or for luminescence imaging) if such complexes are highly stable under physiological conditions. Therefore, the complex with the particular metal ion must be thermodynamically stable and the ligand as selective as possible in a class of competing metal ions. However, it is now commonly recognized that kinetic inertness to dissociation of such complexes is also very important and is usually decisive for stability *in vivo*. Use of metal radioisotopes has raised another requirement—very fast complexation of short-living radioisotopes to enable to use of the isotopes in the kit form in hospitals.

<sup>a</sup>Department of Analytical Chemistry, Masarykova universita (Masaryk University), Kotlářská 2, Brno, 602 00, Czech Republic. E-mail: lubal@chemi.muni.cz; Fax: +420-54949-2494; Tel: +420-54949-5637

<sup>b</sup>Department of Inorganic Chemistry, Universita Karlova (Charles University), Hlavova 2030, Prague 2, 128 40, Czech Republic. E-mail: petr@natur.cuni.cz; Fax: +420-22195-1253; Tel: +420-22195-1263

† Electronic supplementary information (ESI) available: Figures of speciation in some M<sup>2+</sup>–H<sub>4</sub>L, H<sup>+</sup>–H<sub>4</sub>L and M<sup>2+</sup>–OH<sup>–</sup> systems, crystal packing in structure of the Zn(II) and Mn(II) complexes, disorder simulation in structure of the Mn(II) complex, figure showing crystal structure of H<sub>4</sub>L, examples of dependence of experimental <sup>1</sup>k<sub>obs</sub> on c<sub>Zn</sub> or c<sub>Cd</sub>, tables with kinetic experimental data. See DOI: 10.1039/b603251f

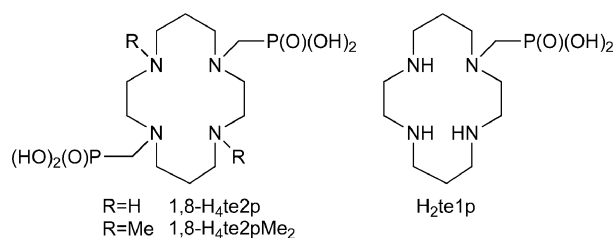
From the viewpoint of thermodynamic stability and dissociation inertness, the macrocyclic ligands are more suitable for utilization of their metal complexes in medicine than the open-chain chelators. However, they often exhibit very slow complex formation kinetics in contrast to fast complexation with open-chain ligands (e.g. H<sub>3</sub>dtpa and its derivatives). Macrocyclic ligands are mostly derivatives of two parent compounds—H<sub>4</sub>dota and H<sub>4</sub>teta (Scheme 1), derived from well-known cyclic amines, 1,4,7,10-tetraazacyclododecane (cyclen) and 1,4,8,11-tetraazacyclotetradecane (cyclam). H<sub>4</sub>dota forms stable complexes with a number of common metal ions and is suitable for most of them, but preferable for lanthanide(III) ions requiring high coordination numbers.<sup>1–5</sup> H<sub>4</sub>teta is more appropriate for transition-metal ions as a larger ring allows planar coordination of all nitrogen atoms.<sup>1–5</sup> However, such octadentate ligands do not usually utilize all donor atoms for binding to transition-metal ions in mononuclear species and they form polynuclear complexes.



Scheme 1

Many cyclen and cyclam phosphorus acid derivatives (mostly phosphonic acids H<sub>8</sub>dotp and H<sub>8</sub>tetp, Scheme 1) and their complexes have been investigated.<sup>19–21</sup> The phosphonic acid ligands are generally highly basic and, therefore, their complexes show a high thermodynamic stability.<sup>19–26</sup> Stability constants of the complexes of less basic phosphinic acid derivatives (e.g. H<sub>4</sub>dotp<sup>R</sup> and H<sub>4</sub>tetp<sup>R</sup>, Scheme 1) are lower but usually comparable with those of complexes of H<sub>4</sub>dota and H<sub>4</sub>teta.<sup>27–29</sup>

Some time ago, we have started investigations of ligands containing fewer phosphorus acid arms as such hexadentate ligands are more suitable for octahedral coordination to the transition-metal ions. Therefore, we decided to synthesize<sup>22</sup> 1,8-bis(phosphonic acid) derivatives of cyclam, namely 1,8-H<sub>4</sub>te2p and 1,8-H<sub>4</sub>te2pMe<sub>2</sub> (Scheme 2), having just six coordinating sites. The presence of phosphonic acid groups also overcomes the undesirable formation of the inner lactam described for an acetate analogue.<sup>30</sup> The *cis*- and *trans*-isomers of nickel(II)<sup>31</sup> and cobalt(III)<sup>32</sup> complexes of 1,8-H<sub>4</sub>te2p (H<sub>4</sub>L) were isolated in several differently protonated forms even such as [Ni(H<sub>4</sub>L)]<sup>2+</sup>, where the



Scheme 2

phosphonic groups are fully protonated and are coordinated only through the phosphoryl oxygen atom.<sup>31</sup> Such coordination was observed for the first time in the solid state. With copper(II), two extremely stable isomeric forms of [Cu(H<sub>2</sub>L)] were isolated.<sup>33</sup> The low-temperature kinetic isomer is five-coordinated with one phosphonic acid pendant arm uncoordinated. It isomerizes on heating to the thermodynamic octahedral isomer with *trans* arrangement of phosphonic acid moieties. As the complexes were intended as models for more sophisticated complexes possibly useful in nuclear medicine, very promising results were obtained from investigation of acid-assisted decomplexation.<sup>33</sup> The octahedral complex is one of the most kinetically inert complexes of copper(II). For both isomers, the slow decomposition may be a consequence of an overall positive charge of complex species on the full protonation of non-coordinated phosphonate oxygen atoms.<sup>33</sup> We proved that the complexation of copper(II) by the ligand is highly selective and we employed the property in an efficient analytical determination of copper.<sup>34,35</sup> The results show that 1,8-H<sub>4</sub>te2p is one of the ligands most suitable for copper(II) complexation.

As the copper radioisotopes are produced by irradiation of parent nickel or zinc isotopes,<sup>13</sup> nickel(II) or zinc(II) ions are the most common chemical impurities in commercial sources of copper radioisotopes. For this reason, special selectivity for copper(II) complexation over the zinc(II) or nickel(II) binding is required.

In our previous studies, we focused on complexing behaviour of 1,8-H<sub>4</sub>te2p with transition-metal ions (Cu<sup>2+</sup>, Ni<sup>2+</sup>, Co<sup>3+</sup>).<sup>31–35</sup> Here, we report on the thermodynamic studies of 1,8-H<sub>4</sub>te2p complexes with divalent transition-metal ions as well as with alkaline-earth ions. Three new crystal structures of the complexes are reported. In addition, we report on the formation and dissociation kinetics of zinc(II) and cadmium(II) complexes of the title ligand.

## Experimental

### Materials

The ligand, 1,8-H<sub>4</sub>te2p·4H<sub>2</sub>O (H<sub>4</sub>L·4H<sub>2</sub>O), was synthesized by the method described elsewhere.<sup>22</sup> Analytical grade chemicals were purchased from Lachema (Czech Republic), Fluka or Merck and were used as received. For potentiometric titrations, metal nitrates or MnSO<sub>4</sub>·4H<sub>2</sub>O (recrystallized from deionized water) were used and their stock solutions were standardized by titration with Na<sub>2</sub>H<sub>2</sub>edta according to the recommended procedure.<sup>36</sup> The stock solution of nitric acid (~0.03 mol dm<sup>-3</sup>) was prepared from recrystallized KNO<sub>3</sub> on ion-exchange resin (Dowex 50). Diluted HNO<sub>3</sub> obtained by this way is more pure than that prepared from conc. HNO<sub>3</sub> as the concentrated acid contains traces of NO<sub>x</sub>. Carbonate-free KOH stock solution (~0.2 mol dm<sup>-3</sup>) was prepared from potassium metal (Aldrich) under argon atmosphere. The hydroxide solution was standardized against potassium hydrogen phthalate and the HNO<sub>3</sub> solution against the ~0.2 mol dm<sup>-3</sup> KOH solution. The analytical grade chemicals employed in the kinetic studies were purchased from Lachema (ZnCl<sub>2</sub>, CdCl<sub>2</sub>·6H<sub>2</sub>O, KOH, CH<sub>3</sub>COOH) and Fluka (2-morpholine-ethanesulfonic acid, MES). The indicators bromocresol green (Lachema), bromocresol purple (Merck) and 4-(2-pyridylazo)resorcinol (PAR, Lachema) were of the highest available purity. The freshly prepared solutions of CdCl<sub>2</sub> and ZnCl<sub>2</sub>

were standardized chelatometrically at pH ~9.2 (ammonia buffer) against Eriochrom black T.

### Potentiometric titrations

The equilibria in ligand : metal systems with all metal ions except for  $\text{Co}^{2+}$  and  $\text{Ni}^{2+}$  were established in the course of minutes in each titration point and, thus, they could be studied by conventional titrations. The titrations were carried out in a thermostatted vessel at  $25.0 \pm 0.1$  °C, at constant ionic strength  $I(\text{KNO}_3) = 0.1 \text{ mol dm}^{-3}$ , using a PHM 240 pH-meter, a 2 ml ABU 900 automatic piston burette and a GK 2401B combined glass electrode (all Radiometer). The ligand concentration in the titration vessel was *ca.*  $0.004 \text{ mol dm}^{-3}$ . The ligand-to-metal ratio was 1 : 1 in all cases. The initial volume was *ca.* 5 ml. The measurements were taken with a  $\text{HNO}_3$  excess added to the mixture. The mixtures were titrated with the stock KOH solution in the region of  $-\log[\text{H}^+] = 1.6\text{--}12.0$ . Titrations for each system were carried out at least four times. Each titration consisted of *ca.* 40 points. Inert atmosphere was provided by constant passage of argon saturated with water vapour. The complexation reaction was too slow to be followed by standard titrations for systems with  $\text{Co}^{2+}$  and  $\text{Ni}^{2+}$ . These systems were studied by the “out-of-cell” method. Each titration consisted of *ca.* 25 solutions (two parallel titrations), each solution was mixed separately in the test tube (each sample volume *ca.* 1 ml) and an appropriate amount of the KOH solution was added to each test tube to simulate the common titration. The tubes were tightly closed and left to equilibrate for two days ( $\text{Co}^{2+}$ ) or three weeks ( $\text{Ni}^{2+}$ ). These equilibration times were determined in separate preliminary experiments. Then, the potential at each titration point (tube) was determined with freshly calibrated electrode.

The constants with their standard deviations were calculated using the OPIUM program package.<sup>37</sup> The program minimises the criterion of the generalised least-squares method using the calibration function given in eqn (1).

$$E = E_0 + S \log[\text{H}^+] + j_1[\text{H}^+] + j_2 K_w / [\text{H}^+] \quad (1)$$

The term  $E_0$  contains the standard potentials of the electrodes used and the contributions of inert ions to the liquid-junction potential. The term  $S$  corresponds to the Nernstian slope and the terms  $j_1[\text{H}^+]$  and  $j_2 K_w / [\text{H}^+] = j_2 \times [\text{OH}^-]$  are contributions of the  $\text{H}^+$  and  $\text{OH}^-$  ions to the liquid-junction potential. It is clear that  $j_1$  and  $j_2$  cause a deviation from a linear dependence of  $E$  and  $-\log[\text{H}^+]$  only in strongly acidic and alkaline solutions. The calibration parameters were determined from titration of the standard  $\text{HNO}_3$  with the standard KOH solutions before and after every titration of the ligand/metal ion system to give calibration–titration pairs used for calculations of stability constants. The concentration dissociation constants  $K_a$  of 1,8-H<sub>4</sub>te2p ( $\text{H}_4\text{L}$ ) were taken from the literature.<sup>22</sup> The stability constants  $\beta_{hlm}$  are defined as  $\beta_{hlm} = [\text{H}_h\text{L}_l\text{M}_m] / ([\text{H}]^h [\text{L}]^l [\text{M}]^m)$ . The water ion product  $\text{p}K_w$  taken for calculations was 13.78. Stability constants of metal hydroxo complexes included in the calculations were taken from literature.<sup>38–40</sup>

### Kinetic measurements

All experiments were made at a temperature  $25.0 \pm 0.2$  °C. The ionic strength  $0.1 \text{ mol dm}^{-3}$  was maintained with KCl. The final

pH of the buffered solution was checked by a pH-meter calibrated with standard buffers.

The formation kinetics of  $\text{Cd}^{2+}$  and  $\text{Zn}^{2+}$  complexes were followed under pseudo-first-order conditions ( $c(\text{MCl}_2) = (1\text{--}10) \times 10^{-3} \text{ mol dm}^{-3}$ ,  $c(\text{H}_4\text{L}) = 1 \times 10^{-4} \text{ mol dm}^{-3}$ ) in the pH (pH-meter calibrated with standard buffers) range 3.7–6.8 ( $\text{Zn}^{2+}$ ) and 4.6–7.0 ( $\text{Cd}^{2+}$ ); the indicator technique was used for detection of the reaction course.<sup>41</sup> The formation kinetics of the  $\text{Cu}^{2+}$  complex was followed in the pH range 5.0–7.0 analogously to a published procedure (stopped-flow measurements).<sup>33</sup> The reactions were performed in slightly buffered solution ( $0.005 \text{ mol dm}^{-3}$  potassium acetate/acetic acid or MES acid/ $\text{K}^+$ -salt buffers) and the  $2 \times 10^{-5} \text{ mol dm}^{-3}$  solution of indicator (bromocresol green (pH < 5.2) or bromocresol purple (pH > 5.2)) was used for visualization.

The dissociation kinetics of  $[\text{Zn}(\text{L})]^{2-}$  and  $[\text{Cd}(\text{L})]^{2-}$  complexes ( $c = 1 \times 10^{-3} \text{ mol dm}^{-3}$ ) were measured in the pH range 3.7–4.8 (zinc(II) complex) and 4.5–6.1 (cadmium(II) complex) and in  $I = 0.1 \text{ mol dm}^{-3}$ . The reactions were performed in buffered solution ( $0.05 \text{ mol dm}^{-3}$  potassium acetate/acetic acid or MES acid/ $\text{K}^+$ -salt buffers). For both complexes,  $\text{Cu}^{2+}$  ion ( $c(\text{CuCl}_2) = 1 \times 10^{-3} \text{ mol dm}^{-3}$ ,  $\lambda_{\text{max}} = 310 \text{ nm}$ ) was used as a ligand scavenger. For the  $[\text{Zn}(\text{L})]^{2-}$  complex, 4-(2-pyridylazo)resorcinol (PAR) ( $c(\text{PAR}) = 2 \times 10^{-5} \text{ mol dm}^{-3}$ ,  $\lambda_{\text{max}} = 498 \text{ nm}$ ) was also utilized as a zinc(II) scavenger. It was verified (by checking of formation kinetics under our experimental conditions) that the visualisation reaction between the ligand or the metal ion and their scavengers was much faster than dissociation reaction of the studied complexes (for complexation kinetics of  $\text{Cu}^{2+}$  ion with  $\text{H}_4\text{L}$ , see also ref. 33). Dissociation kinetics was performed at different copper(II) concentrations to verify a direct transchelation reaction. No dependence of  $k_{\text{obs}}$  on  $c_{\text{Cu}}$  was observed (Table S5, ESI†). It confirms that complex dissociation is the rate-determining step followed by fast complexation with the scavenger.<sup>42</sup> Therefore, the transchelation can be neglected in further treatment of the experimental data.

The kinetic measurements were carried out on diode-array spectrophotometer HP 8453A (Hewlett Packard, USA) for slow kinetics ( $10\tau_{1/2} > 10 \text{ min}$ ) and on a Bio Sequential SX-17 stopped-flow spectrometer (Applied Photophysics, UK) for fast kinetics ( $10\tau_{1/2} < 10 \text{ min}$ ). The measured values of absorbance were corrected for the background analytical signal. Values of  $k_{\text{obs}}$  were obtained from experimental data by HP software and Excel<sup>43</sup> software with identical results. The dependence of  $k_{\text{obs}}$  on proton concentration were treated with Excel software.<sup>43</sup>

### Preparation of single crystals

**trans-O<sub>2</sub>O-[Zn(H<sub>2</sub>L)].** A solution of  $\text{H}_4\text{L} \cdot 4\text{H}_2\text{O}$  (50 mg, 0.11 mmol) in water (5 ml) was mixed with a solution of  $\text{Zn}(\text{OAc})_2 \cdot 2\text{H}_2\text{O}$  (24 mg, 0.11 mmol) in water (5 ml) and the mixture was sealed in a vial. The solution was heated to *ca.* 90 °C and held at this temperature overnight. Small colourless prisms of the product suitable for X-ray structure determination were formed on the walls of the vial. Yield ~70%.

**[{(H<sub>2</sub>O)<sub>5</sub>Mn}<sub>2</sub>(μ-H<sub>2</sub>L)](H<sub>2</sub>L)·21H<sub>2</sub>O.** The ligand hydrate (50 mg, 0.11 mmol) and  $\text{MnCO}_3$  (12.6 mg, 0.11 mmol) were added to water (5 ml) and refluxed under argon for 72 h (until  $\text{MnCO}_3$  completely dissolves). The light yellow solution was then filtered and concentrated under vacuum to *ca.* 1 ml; pH of the

solution was *ca.* 5.5. On standing for several days, light yellow single crystals of the product appeared. Yield ~30%.

**[Pb(H<sub>2</sub>L)(H<sub>2</sub>O)<sub>2</sub>]-6H<sub>2</sub>O.** A solution of H<sub>4</sub>L·4H<sub>2</sub>O (50 mg, 0.11 mmol) in water (5 ml) was mixed with a solution of Pb(OAc)<sub>2</sub>·3H<sub>2</sub>O (39 mg, 0.11 mmol) in water (5 ml); pH of the solution was *ca.* 5. The solution was then evaporated under vacuum and the white residue was redissolved in water (1.5 ml). Colorless prisms of the product suitable for X-ray structure determination were formed on standing over several days. Yield ~35%.

### Crystallography

Selected crystals were quickly transferred from the mother-liquor into Fluorolub oil, mounted on glass fibres in random orientation and cooled to 150(1) K. Diffraction data were collected using a Nonius Kappa CCD diffractometer (Enraf-Nonius) at 150(1) K (Cryostream Cooler, Oxford Cryosystem) using Mo-K $\alpha$  radiation ( $\lambda = 0.71073$  Å) and analyzed using the HKL program package.<sup>44</sup> The structures were solved by direct methods and refined by full-matrix least-squares techniques (SIR92 (ref. 45) and SHELXL97 (ref. 46)). Scattering factors for neutral atoms used were included in the SHELXL97 program. Table 1 gives pertinent crystallographic data.

In the structure of *trans*-O,O-[Zn(H<sub>2</sub>L)], the asymmetric unit consists of two independent halves of the complex molecule. Zinc atoms are located on the inversion centres. All non-hydrogen atoms were refined anisotropically. The hydrogen atoms were located in the electron density difference map. Nevertheless, hydrogens

attached to carbon atoms were fixed in theoretical positions. Hydrogen atoms bound to nitrogen and oxygen atoms were refined isotropically.

In the structure of {[Pb(H<sub>2</sub>L)(H<sub>2</sub>O)<sub>2</sub>]-6H<sub>2</sub>O}<sub>n</sub>, the metal ion and two halves of the macrocyclic ligand form the asymmetric unit. All non-hydrogen atoms except those belonging to two co-crystallized water molecules were refined anisotropically. All hydrogen atoms attached to carbon, nitrogen or coordinated oxygen atoms were located in the electron difference map; however, they were fixed in theoretical or original positions with thermal parameters  $U_{\text{eq}}(\text{H}) = 1.2U_{\text{eq}}(\text{C})$  or  $1.3U_{\text{eq}}(\text{N},\text{O})$  as the free refinement led to unrealistic bond lengths. Some hydrogen atoms belonging to co-crystallized water molecules were also found and were treated using AFIX 3 instruction and  $U_{\text{eq}}(\text{H}) = 1.3U_{\text{eq}}(\text{O})$ . Two oxygen atoms of water molecules were found disordered in several positions, and they were refined isotropically. Overall, the quality of the diffraction data was rather poor, probably due to a presence of several small crystallites on the main single crystal. Therefore, no successful absorption correction could be applied, which lead to a relatively big peak-and-hole difference (6.6 and  $-3.2 \text{ e } \text{Å}^{-3}$ ); they are located very close to the lead atom (0.81 and 0.68 Å, respectively).

The independent unit of [(H<sub>2</sub>O)<sub>5</sub>Mn]<sub>2</sub>( $\mu$ -H<sub>2</sub>L)(H<sub>2</sub>L)·21H<sub>2</sub>O consists of the penta-aquamanganese(II) moiety coordinated by one oxygen atom of the pendant phosphonate belonging to one half of the ligand molecule (there is a centre of symmetry lying inside the macrocycle cavity). The other independent half of molecule of the ligand is not coordinated and serves as a counter anion and the macrocyclic part of this uncoordinated ligand molecule is highly disordered. This disorder was best described by

**Table 1** Experimental and refinement data for the X-ray diffraction studies

Parameter	<i>trans</i> -O,O-[Zn(H <sub>2</sub> L)]	[Pb(H <sub>2</sub> L)(H <sub>2</sub> O) <sub>2</sub> ]-6H <sub>2</sub> O	[(H <sub>2</sub> O) <sub>5</sub> Mn] <sub>2</sub> ( $\mu$ -H <sub>2</sub> L)(H <sub>2</sub> L)·21H <sub>2</sub> O
Empirical formula	C <sub>12</sub> H <sub>28</sub> N <sub>4</sub> O <sub>6</sub> P <sub>2</sub> Zn	C <sub>12</sub> H <sub>44</sub> N <sub>4</sub> O <sub>14</sub> P <sub>2</sub> Pb	C <sub>24</sub> H <sub>118</sub> Mn <sub>2</sub> N <sub>8</sub> O <sub>43</sub> P <sub>4</sub>
$M_r$	451.69	737.64	1441.02
$T/\text{K}$	150(1)	150(1)	150(1)
Crystal dimensions/mm	0.20 × 0.13 × 0.10	0.40 × 0.20 × 0.13	0.20 × 0.13 × 0.10
Shape	Prism	Prism	Prism
Colour	Colourless	Colourless	Pale yellow
Crystal system	Triclinic	Triclinic	Triclinic
Space group	$P\bar{1}$ (no. 2)	$P\bar{1}$ (no. 2)	$P\bar{1}$ (no. 2)
$a/\text{Å}$	9.4638(7)	10.029(1)	9.7361(3)
$b/\text{Å}$	9.5509(6)	10.416(1)	12.2695(4)
$c/\text{Å}$	11.1074(8)	14.322(1)	14.0948(4)
$\alpha/^\circ$	89.068(4)	77.055(2)	87.808(2)
$\beta/^\circ$	88.094(3)	73.698(2)	77.378(2)
$\gamma/^\circ$	60.882(3)	71.776(2)	88.4157(13)
$V/\text{Å}^3$	876.61(11)	1348.6(2)	1641.51(9)
$Z$	2	2	1
$D_c/\text{g cm}^{-3}$	1.711	1.817	1.458
$\mu/\text{mm}^{-1}$	1.622	6.444	0.584
$F(000)$	472	756	772
$\theta$ Range of data collection/ $^\circ$	3.05–27.53	3.29–27.65	2.96–27.51
Index ranges, $hkl$	–12 to 12, –12 to 12, –13 to 14	–12 to 13, –13 to 13, –18 to 18	–12 to 12, –15 to 15, –18 to 18
Reflections measured	3913	6088	7504
Reflections observed [ $I > 2\sigma(I)$ ]	2973	5864	5560
Data, restraints, parameters	3913, 0, 341	6088, 0, 303	7504, 0, 406
Goodness-of-fit on $F^2$	1.039	1.159	1.040
$R, R'$ indices [ $I > 2\sigma(I)$ ] <sup>a</sup>	0.0743, 0.0522	0.0473, 0.0453	0.0755, 0.0485
$wR, wR'$ [ $I \geq 2\sigma(I)$ ] <sup>a</sup>	0.1405, 0.1265	0.1033, 0.1022	0.1224, 0.1080
Maximum shift/esd	0.001	0.001	0.007
$\Delta\rho_{\text{max, min}}/\text{e } \text{Å}^{-3}$	1.199, –0.829	6.576, –3.228	0.983, –0.903

<sup>a</sup>  $w = 1/[\sigma^2(F_o^2) + (AP)^2 + BP]$ ,  $P = (F_o^2 + 2F_c^2)/3$  (ref. 46) and  $R, R' = \sum |F_o - F_c| / \sum |F_c|$ ;  $wR, wR' = [\sum w(F_o^2 - F_c^2)^2 / \sum w(F_o^2)^2]^{1/2}$  (ref. 46).

placing of part of macrocycle into two positions with occupancies approximately 63 : 37. However, both conformations are very similar (Fig. S5, ESI†). As some C–C distances became too long during a free refinement they were treated using DFIX command; however, it lead to very prolate thermal ellipsoids with large max./min. ratio of anisotropic displacement parameters (up to 8.5), indicating possibly a more complicated disorder. Additionally, 10 water molecules of crystallization were found in the independent unit and the 11th was best refined with half-occupancy. In the pentaquamanganese(II) unit, one of the coordinated water molecules was found to be disordered in two positions and was refined isotropically with relative occupancies 77 : 23. Other non-hydrogen atoms were refined anisotropically. The hydrogen atoms belonging to the carbon or nitrogen atoms of the coordinating ligand molecule or to co-crystallized water molecules were located in electron difference map, but they were fixed in theoretical positions with thermal parameters  $U_{\text{eq}}(\text{H}) = 1.2U_{\text{eq}}(\text{C})$  or  $1.3U_{\text{eq}}(\text{N})$  or kept in the original geometry using AFIX 3 instruction with  $U_{\text{eq}}(\text{H}) = 1.3U_{\text{eq}}(\text{O})$ ; the free refinement lead to unrealistic bond lengths and values of thermal parameters. The hydrogen atoms of the disordered uncoordinated ligand molecule were fixed in theoretical positions using the same riding model.

CCDC reference numbers 600826–600828.

For crystallographic data in CIF or other electronic format see DOI: 10.1039/b603251f

## Results and discussion

### Thermodynamic stability of metal complexes

As expected, values of stability constants of alkaline earth metal ions are low (Table 2); nevertheless, differences in titration curves of the pure ligand and of ligand– $\text{M}^{2+}$  systems are different (Fig. S1, ESI†) and the constants were determined with satisfactory precision. Complexation of the metal ions starts in slightly acid region ( $-\log[\text{H}^+]$  5–6) by formation of low-abundant (~20%) diprotonated  $\text{H}_2\text{LM}$  species (representative distribution diagrams for  $\text{Mg}^{2+}$  and  $\text{Ca}^{2+}$  systems are shown in Fig. S2, ESI†). Protons from the species (as well as from the free ligand) are removed only in highly alkaline solutions and, thus, the species with LM

stoichiometry have a reasonable abundance only in the strong alkaline region ( $-\log[\text{H}^+] > 10$  for  $\text{Mg}^{2+}$  and  $> 12$  for  $\text{Ca}^{2+}$ ,  $\text{Sr}^{2+}$  and  $\text{Ba}^{2+}$ ). It also corresponds to  $\text{p}K_{\text{a}}$  values related with deprotonations of the  $\text{H}_2\text{LM}$  and  $\text{HLM}$  species (Table 2,  $\text{p}K_{\text{a}} = 10.8$ – $12.1$ ). They are much higher than those corresponding to deprotonation(s) of the phosphonate moieties ( $\text{p}K_{\text{a}} = 5.36$  ( $\text{H}_4\text{L}$ ) and  $6.78$  ( $\text{H}_3\text{L}$ )) and lower than those assigned to deprotonations of  $>\text{NH}_2^+$  groups ( $\text{p}K_{\text{a}} \sim 13.2$  for the  $\text{H}_2\text{L}/\text{HL}$  species) of the free ligand. One can attribute deprotonations of the  $\text{H}_2\text{LM}$  and  $\text{HLM}$  species to the proton dissociations from secondary amino groups of the macrocycle. Thus, the metal ions would be bound only by oxygen atoms of the pendant groups in the double-protonated  $\text{H}_2\text{LM}$  species and coordination of nitrogen atoms can occur only in  $\text{LM}$  (and possibly also in  $\text{HLM}$ ) species. Among alkaline earth ions, it is clearly seen that the ligand is selective for  $\text{Mg}^{2+}$  (unlike  $\text{H}_4\text{L}$ ) as a consequence of a higher affinity of phosphonates to the small hard cation.

Previously, we have proved<sup>31,32,33</sup> for  $\text{Ni}^{2+}$ ,  $\text{Co}^{2+}/\text{Co}^{3+}$  and  $\text{Cu}^{2+}$  ions that only kinetic (*cis*-O,O or pentacoordinated, respectively) isomers are formed at room temperature and all nitrogen atoms are bound in these complexes. Therefore, *cis*-O,O arrangement is expected for the highly stable complexes (Table 2) of transition-metal ions ( $\text{Co}^{2+}$ ,  $\text{Ni}^{2+}$ ,  $\text{Zn}^{2+}$  and  $\text{Cd}^{2+}$ ) formed during potentiometric titrations. Complexation starts in the acid solutions (Fig. 1 and S2, ESI†) and we assume coordination of the macrocyclic ring nitrogen atoms even in acid region. This is supported by values of  $\text{p}K_{\text{a}}$  corresponding to deprotonation of the  $\text{H}_2\text{LM}$  and  $\text{HLM}$  species (Table 2) as they are much lower than values corresponding to the last two proton dissociations from the free ligand and are more comparable with those for proton dissociations from phosphonate moieties of the free ligand. The acidity of  $\text{H}_2\text{LM}$  species is mostly higher ( $\text{p}K_{\text{a}}$  in the range 4.5–5.6) in comparison with that of the  $\text{PO}_3\text{H}^-$  moieties of the free ligand (5.36, 6.78) indicating coordination of the pendant group(s) as their acidity is increased due to the electron-withdrawing effect of the metal ion when bound. However, the acidity of the  $\text{HLM}$  species is lower ( $\text{p}K_{\text{a}}$  in the range 7.2–7.8) than that of the last  $\text{PO}_3\text{H}^-$  moiety in the free ligand ( $\text{p}K_{\text{a}}$  corresponding to this proton dissociation is 6.78). This effect can be attributed to a presence of an intramolecular hydrogen bond between coordinated pendant arms ( $-\text{PO}_3^{2-}$  and  $-\text{PO}_3\text{H}^-$ ) which is possible only in a *cis*-O,O

**Table 2** Stability constants of metal ion complexes with 1,8- $\text{H}_4\text{te}2\text{p}^a$  (25 °C,  $I = 0.1 \text{ mol dm}^{-3} \text{ KNO}_3$ )

Equilibrium <sup>b</sup>	<i>hlm</i>	$\text{Mg}^{2+}$	$\text{Ca}^{2+}$	$\text{Sr}^{2+}$	$\text{Ba}^{2+}$	$\text{Mn}^{2+}$	$\text{Co}^{2+}$	$\text{Ni}^{2+}$	$\text{Cu}^{2+c}$	$\text{Zn}^{2+}$	$\text{Cd}^{2+}$	$\text{Pb}^{2+}$
		$\log \beta_{lm}$										
$\text{M} + \text{L} \rightleftharpoons \text{ML}$	011	8.61(5)	5.26(3)	4.09(4)	3.90(13)	12.35(3)	19.28(6)	21.99(8)	25.40	20.35(4)	17.89(3)	14.96(3)
$\text{H} + \text{L} + \text{M} \rightleftharpoons \text{HML}$	111		16.93(6)		16.39(7)	21.22(4)	27.09(3)	29.30(5)	32.45	27.52(2)	25.45(1)	23.97(1)
$2\text{H} + \text{L} + \text{M} \rightleftharpoons \text{H}_2\text{ML}$	211	28.35(9)	28.43(5)	28.30(8)	28.01(11)		31.57(7)	34.07(3)	37.55	31.96(5)	31.04(2)	29.72(4)
$3\text{H} + \text{L} + \text{M} \rightleftharpoons \text{H}_3\text{ML}$	311					35.1(1)						
		$\text{p}K_{\text{a}}$										
$\text{H}_2\text{ML} \rightleftharpoons \text{HML} + \text{H}$			11.50		11.6		4.48	4.77	5.10	4.44	5.59	5.75
$\text{HML} \rightleftharpoons \text{ML} + \text{H}$			11.67		12.49	8.87	7.81	7.31	7.05	7.17	7.56	9.01
$\text{H}_2\text{ML} \rightleftharpoons \text{ML} + 2\text{H}$		19.74		24.21								
$\text{H}_3\text{ML} \rightleftharpoons \text{HML} + 2\text{H}$						13.9						

<sup>a</sup> Dissociation constants<sup>22</sup> of 1,8- $\text{H}_4\text{te}2\text{p} = \text{H}_4\text{L}$ :  $\text{p}K_{\text{H}_4\text{L}} + \text{p}K_{\text{H}_3\text{L}} = 26.41$ ;  $\text{p}K_{\text{H}_3\text{L}} = 6.78$ ;  $\text{p}K_{\text{H}_2\text{L}} = 5.36$ ;  $\text{p}K_{\text{H}_2\text{L}} = 1.15$ . <sup>b</sup> Charges are omitted for clarity.

<sup>c</sup> Values for pentacoordinated complex; taken from ref. 33.

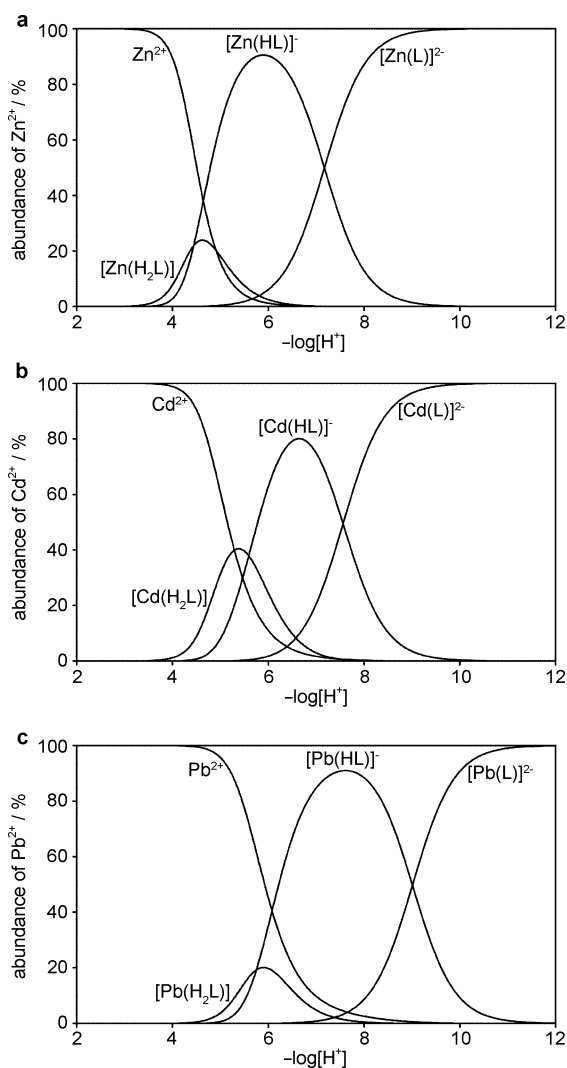


**Fig. 1** Distribution diagrams of  $M^{2+}$ -1,8- $H_4te2p$  systems ( $c_M = c_L = 0.004 \text{ mol dm}^{-3}$ );  $M = \text{Zn}$  (a),  $\text{Cd}$  (b) and  $\text{Pb}$  (c).

arrangement assumed for these species. Such a hydrogen bond would stabilize the last proton and it would lead to an increase in  $pK_a$  value assigned to the proton dissociation. A difference in  $pK_a$  values for the *cis*-O,O-[Co<sup>III</sup>(HL)] complex (6.98) exhibiting

much higher  $pK_a$  than its *trans*-O,O-[Co<sup>III</sup>(HL)] isomer (2.97) has been explained by presence of the intramolecular hydrogen bond in the *cis* isomer.<sup>32</sup> The intramolecular hydrogen bond was found in the solid-state structures of the *cis*-O,O-[Co<sup>III</sup>(HL)]<sup>32</sup> and *cis*-O,O-[Ni(H<sub>2</sub>L)]<sup>31</sup> complexes. In addition, acid–base titration of the prepared solid *cis*-O,O-[Ni(H<sub>2</sub>L)] complex (employing a high kinetic inertness of the complex in acid solution) led to identical dissociation constants for the H<sub>2</sub>LNi and HLNi species (4.78 and 7.35, respectively).<sup>31</sup> It is an indirect proof that structures of the complex in the solid state and the species present in solution under equilibrium conditions (this paper) should be identical. Therefore, we assume *cis* coordination of the pendant groups in the complexes of the transition-metal ions. On the other hand, Cu<sup>2+</sup> forms at room temperature pentacoordinated species (N<sub>4</sub>O coordination mode) and the corresponding  $pK_a$  value (7.05) was attributed to deprotonation of the uncoordinated phosphonate.<sup>33</sup>

A comparison of abundances of various forms of Zn<sup>2+</sup> and Cd<sup>2+</sup> complexes (relevant to kinetic studies, see below) is shown in Fig. 1. The highest stability was found for the copper(II) complex<sup>33</sup> (Table 3) and it reflects the usual Irving–Williams trend and optimal size of the fourteen-membered macrocyclic cavity for divalent copper.<sup>17,47,48</sup> The ligand is highly selective for Cu<sup>2+</sup> (but less than cyclam itself) and the property has been explored in analytical determination of the ion in the presence of a range of competing ions.<sup>34,35</sup> In comparison with H<sub>4</sub>teta, there are much larger differences in values of stability constants of 1,8- $H_4te2p$  with most of the divalent metal ions studied.

The behaviour of divalent manganese and lead complexes is just on borderline. Both the metal ions have a higher affinity to harder oxygen donor atoms. In the H<sub>2</sub>LM species, they should be bound to phosphonate moiety(ies) with double-protonated ring nitrogen atoms. This is supported by  $pK_a$  values corresponding to the HLM species (9.01 and 8.87 for Pb<sup>2+</sup> and Mn<sup>2+</sup>, respectively) and structure of the complexes isolated in the solid state (see below). The neutral solid complexes (having H<sub>2</sub>LM stoichiometry) were isolated in the pH region where the protonated species are present. Binding of nitrogen atom(s) should be assumed in the ML species. Such behaviour is a consequence of the high basicity of the nitrogen atoms in the free ligand and a relatively high donor ability of the deprotonated phosphonate moiety(ies). Distribution diagrams for Pb<sup>2+</sup> and Mn<sup>2+</sup>-1,8- $H_4te2p$  systems are shown in Fig. 1 and S2, ESI,<sup>†</sup> respectively.

**Table 3** Comparison of stability constants ( $\log \beta_{011}$ ) of metal complexes of 1,8- $H_4te2p$  with those of related ligands

ion	1,8- $H_4te2p$	Cyclam <sup>38</sup>	H <sub>2</sub> te1p <sup>49</sup>	H <sub>8</sub> te2p <sup>50</sup>	H <sub>4</sub> te2p <sup>Ph 29</sup>	H <sub>4</sub> teta <sup>51,52</sup>
Mg <sup>2+</sup>	8.61	—	5.39	—	—	1.97
Ca <sup>2+</sup>	5.26	—	3.07	—	—	8.4
Sr <sup>2+</sup>	4.09	—	—	—	—	5.82
Ba <sup>2+</sup>	3.90	—	—	—	—	4.1
Mn <sup>2+</sup>	12.35	—	11.81	10.8	—	11.3
Co <sup>2+</sup>	19.28	14.3	—	—	—	16.6
Ni <sup>2+</sup>	21.99	22.2	—	—	—	19.91
Cu <sup>2+</sup>	25.40 ( <i>pc</i> ) <sup>a33</sup> 26.50 ( <i>trans</i> ) <sup>b33</sup>	28.1	27.3	26.6 25.99 <sup>53</sup>	17.19	21.7
Zn <sup>2+</sup>	20.35	15.2	21.07	17.6	9.79	16.40
Cd <sup>2+</sup>	17.89	11.3	15.91	16.7	9.91	18.0
Pb <sup>2+</sup>	14.96	10.9	—	15.5	—	14.3

<sup>a</sup> *pc* means kinetic pentacoordinated species. <sup>b</sup> Thermodynamic *trans*-O,O octahedral species.

To test the chemical model found by potentiometry we carried out some NMR measurements on magnesium(II)- and lead(II)-H<sub>4</sub>L systems. Under conditions used for potentiometry (0.004 M, room temperature), only <sup>31</sup>P NMR spectra could be recorded. Unfortunately, in all tested pH values from 4 up, only rather broad nondiagnostic peaks were obtained. It is probably caused by some equilibria of coordinated–non-coordinated forms of the ligand and/or by equilibria between different conformation of the complexes if the ligand is fully bound. Unfortunately, no signal(s) for <sup>207</sup>Pb could be detected. At higher concentrations (0.01–0.1 M, to improve signal-to-noise ratio mainly for <sup>207</sup>Pb NMR), the <sup>31</sup>P NMR spectra above pH ~4 were again broad or gave more signals (probably the consequence of a presence of more isomeric species). More important, samples with the higher concentration of reactants precipitated at pH > 4.5–5 for Pb<sup>2+</sup> and pH > 7 for Mg<sup>2+</sup>. These partial NMR results indirectly prove probable presence of multiple microscopic equilibria and/or more isomers (at higher pH where ring nitrogen atoms are coordinated, *e.g.* as in the Zn<sup>2+</sup>–cyclam system<sup>54</sup>) and, thus, coordination of nitrogen atoms at higher pH. Such a microscopic equilibria (possibly present only on NMR timescale) cannot be, principally, detected by normal potentiometry.

### Zinc(II), lead(II) and manganese(II) complexes in the solid state

All single-crystals were obtained from solutions having pH 5–6 containing the protonated species (according to the distribution diagrams, see Fig. 1 and S2, ESI†). The colourless single crystals of *trans*-O,O-[Zn(H<sub>2</sub>L)] complex were grown hydrothermally by heating an equimolar Zn<sup>2+</sup>–1,8-H<sub>4</sub>te2p mixture at 90 °C. Therefore, the thermodynamic *trans*-isomer was obtained. Single crystals of the {[Pb(H<sub>2</sub>L)(H<sub>2</sub>O)<sub>2</sub>]·6H<sub>2</sub>O}<sub>n</sub> and [(H<sub>2</sub>O)<sub>5</sub>Mn]<sub>2</sub>(μ-H<sub>2</sub>L)(H<sub>2</sub>L)·21H<sub>2</sub>O complexes were obtained by a slow evaporation of their aqueous solutions. Overall H : L : M stoichiometry (number of protons) of the neutral complexes in the solid state corresponds well to distribution diagrams obtained from potentiometric studies; they were crystallized from solutions having pH where protonated species are present. However, such polymeric complexes are hardly expectable in solution and they should be formed only during crystallization.

***trans*-O,O-[Zn(H<sub>2</sub>L)] complex.** The diffraction analysis revealed almost regular octahedral coordination sphere of Zn<sup>2+</sup> cation with *trans* configuration of the pendant moieties (Fig. 2). In the crystal structure, two independent centrosymmetric complex molecules are present; however, the geometries of both molecules are almost the same and, thus, only one of them is shown in Fig. 2. Important distances and angles are given in Table 4. The cyclam ring exhibits the most stable *trans*-III arrangement.<sup>55</sup> The same configuration of the ring was found in the high-temperature isomers of the Ni<sup>2+</sup> (ref. 31) Cu<sup>2+</sup> (ref. 33) and Co<sup>3+</sup> (ref. 32) complexes of 1,8-H<sub>4</sub>te2p. At room temperature, the *cis* isomers are formed (see also above).<sup>31,32</sup> Unfortunately, we were unable to obtain reproducibly any complex with the expected *cis* arrangement in the solid state shortly after mixing and pH adjustment.

Good quality of crystal data allowed us to refine the positions of all hydrogen atoms. In each of the independent units, the acid hydrogen atoms are attached to uncoordinated oxygen atoms of pendant phosphonate O12 stabilizing the structure by strong

**Table 4** Selected geometric parameters of the *trans*-O,O-[Zn(H<sub>2</sub>L)] complex

	Molecule A	Molecule B
Zn1–N1	2.143(4)	2.153(4)
Zn1–N4	2.116(4)	2.111(4)
Zn1–O11	2.138(3)	2.155(3)
P1–O11	1.493(4)	1.496(4)
P1–O12	1.567(3)	1.573(3)
P1–O13	1.493(3)	1.490(3)
P1–C8	1.835(5)	1.829(6)
N1–Zn1–N4	86.1(2)	85.6(2)
N1–Zn1–N1 <sup>a</sup>	180	180
N1–Zn1–N4 <sup>a</sup>	93.9(2)	94.4(2)
N1–Zn1–O11	86.7(1)	85.9(1)
N1–Zn1–O11 <sup>a</sup>	93.3(1)	94.1(1)
N4–Zn1–N4 <sup>a</sup>	180	180
N4–Zn1–O11	92.3(2)	91.7(1)
N4–Zn1–O11 <sup>a</sup>	87.7(2)	88.3(1)
O11–Zn1–O11 <sup>a</sup>	180	180

<sup>a</sup> Equivalent atoms obtained through the centre of symmetry placed in the central zinc atom.

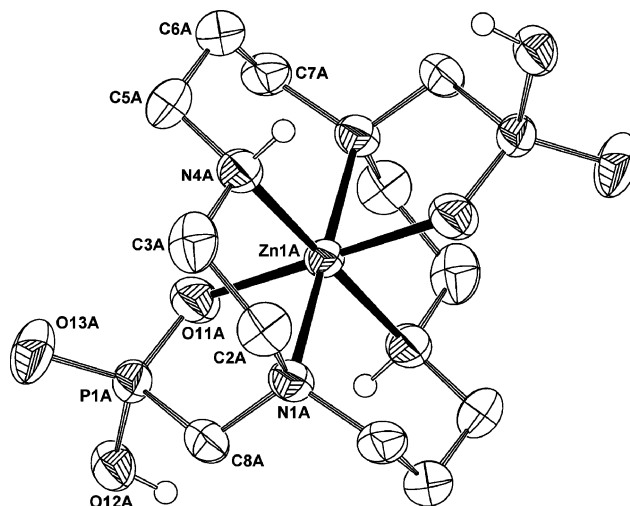


**Fig. 2** Molecular structure of *trans*-O,O-[Zn(H<sub>2</sub>L)] complex with atom numbering scheme. Hydrogen atoms attached to carbon atoms are omitted for clarity.

intermolecular hydrogen bonding with unprotonated O13 oxygen atoms of the neighbouring molecule ( $d(\text{O12}–\text{O13}) = 2.55 \text{ \AA}$  for both independent molecules). Furthermore, the unprotonated oxygen atom O13 is involved in hydrogen binding to secondary amino group (N4,  $d(\text{O13}–\text{N4}) = 3.11$  and  $3.29 \text{ \AA}$  for the independent units). Such intermolecular hydrogen bond network connects the complex molecules in *yz* plane forming a layered structure (Fig. S3, ESI†). As a consequence of the hydrogen bond network, the complex is almost insoluble in water at neutral pH and dissolves only after deprotonation of phosphonate groups at alkaline pH. The octahedron around Zn<sup>2+</sup> is more regular (bond lengths 2.11–2.15 Å and angles 86–94°; Table 4) compared with that in the X-ray crystal structure of [Zn(H<sub>2</sub>teta)]·4H<sub>2</sub>O.<sup>56</sup> The H<sub>4</sub>teta complex represents the same *trans*-III conformation of the ring with two pendant acetate arms uncoordinated and its zinc(II) *trans*-N<sub>4</sub>O<sub>2</sub> octahedron is more distorted with two longer Zn–N bonds (2.25 Å).

**{[Pb(H<sub>2</sub>L)(H<sub>2</sub>O)<sub>2</sub>]-6H<sub>2</sub>O}<sub>n</sub> complex.** The structure is shown in Fig. 3 and all important distances and angles are given in Table 5. The lead(II) ion is coordinated by five oxygen atoms, of which three belong to phosphonate groups and two to water molecules. The Pb–O length for one water molecule is rather long pointing to a very weak coordination (2.99 Å), the second water molecule is coordinated much closer to the metal ion (2.53 Å). The negatively charged phosphonate oxygen atom O11A forms the shortest bond (2.24 Å). The two neighbouring metal ions are connected *via* bridging O11B (the O11B–Pb and O11B–Pb<sup>#</sup> bond distances are 2.32 and 2.49 Å, respectively). The metal ions are separated by 3.93 Å, suggesting no direct metal–metal interaction. The central atom metal ion coordination sphere geometry is very irregular; it could be approximated as an octahedron with one missing vertex

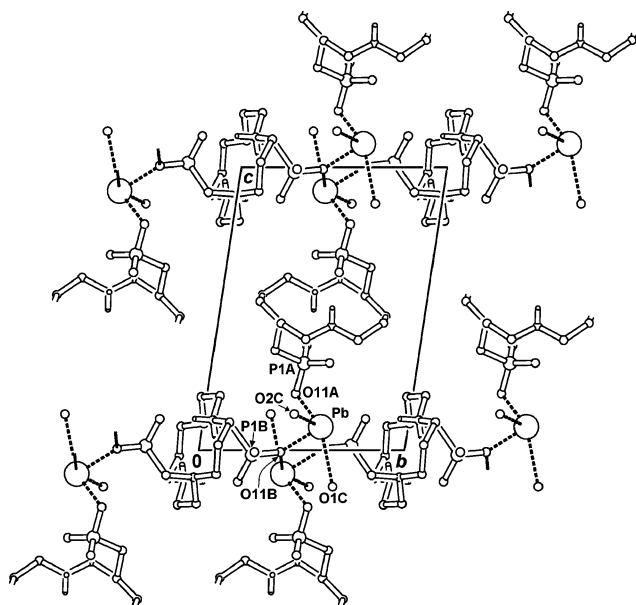


**Fig. 3** The polymeric motif found in the solid-state structure of {[Pb(H<sub>2</sub>L)(H<sub>2</sub>O)<sub>2</sub>]-6H<sub>2</sub>O}<sub>n</sub> complex. The view down to *x* axis. Uncoordinated water molecules and hydrogen atoms attached to carbon atoms are omitted for clarity.

**Table 5** Selected geometric parameters found in the structure of {[Pb(H<sub>2</sub>L)(H<sub>2</sub>O)<sub>2</sub>]-6H<sub>2</sub>O}<sub>n</sub>.

Pb–O11A	2.245(5)	O11A–Pb–O11B	81.2(2)
Pb–O11B	2.318(4)	O11A–Pb–O11B <sup>a</sup>	84.8(2)
Pb–O11B <sup>a</sup>	2.485(5)	O11A–Pb–O1C	151.4(2)
Pb–O1C	2.992(7)	O11A–Pb–O2C	86.4(2)
Pb–O2C	2.525(5)	O11B–Pb–O11B <sup>a</sup>	70.2(2)
Pb–Pb <sup>a</sup>	3.9306(5)	O11B–Pb–O1C	72.2(2)
O <sub>4</sub> -plane–Pb <sup>b</sup>	–0.474(3)	O11B–Pb–O2C	81.3(2)
		O11B <sup>a</sup> –Pb–O1C	76.9(2)
P1A–O11A	1.552(5)	O11B <sup>a</sup> –Pb–O2C	151.2(2)
P1A–O12A	1.524(6)	O1C–Pb–O2C	99.1(2)
P1A–O13A	1.501(5)		
P1A–C8A	1.825(7)		
P1B–O11B	1.550(5)		
P1B–O12B	1.511(5)		
P1B–O13B	1.523(5)		
P1B–C8B	1.821(7)		

<sup>a</sup> Equivalent atoms obtained through the centre of symmetry placed in the middle between the lead atoms. <sup>b</sup> Distance of Pb<sup>2+</sup> ion from the basal plane formed by O1C, O2C, O11A and O11B<sup>#</sup> atoms.

and lead atom lying below the basal O<sub>4</sub>-plane (Table 5). The basal plane is formed by two water O1C and O2C oxygen atoms and by phosphonate O11A and O11B<sup>#</sup> oxygen atoms with O11B atom in the apical position. The neighbouring metal units share O11B and O11B<sup>#</sup> atoms in their basal and apical positions, respectively. The irregular arrangement clearly shows that the free electron pair on lead ion is stereochemically active. The macrocycle is not coordinated and the secondary amino groups are protonated, assuring electroneutrality of the system. The structure indicates that the complex with analogous protonation may be present as 211 species in solution confirming the results obtained by potentiometry (see above).

Coordination of nitrogen atom(s) in lead(II) complexes of (aminomethyl)phosphonic acids is rather rare and it was observed only in several compounds prepared mostly by hydrothermal synthesis.<sup>57</sup> The four-membered (P)–OPb<sub>2</sub>O–(P) rings were found only in three compounds, namely in polymeric lead(II) (aminoalkyl)phosphonic acid complexes<sup>57d,e,58</sup> having similar structural parameters to those of our four-membered ring.

**{(H<sub>2</sub>O)<sub>5</sub>Mn<sub>2</sub>(μ-H<sub>2</sub>L)}(H<sub>2</sub>L)·21H<sub>2</sub>O complex.** The secondary amino groups are protonated and no ring nitrogen atoms are coordinated, similarly to the lead(II) complex (see above). Each pentaquamanganese(II) ion is bound to one oxygen atom of pendant phosphonate groups on the opposite sites of the cycle and, thus, the ligand bridges two manganese atoms forming the [(H<sub>2</sub>O)<sub>5</sub>Mn<sub>2</sub>(μ-H<sub>2</sub>L)]<sup>2+</sup> cation (Fig. 4). The coordination geometry around Mn<sup>2+</sup> is slightly distorted octahedron (Table 6).

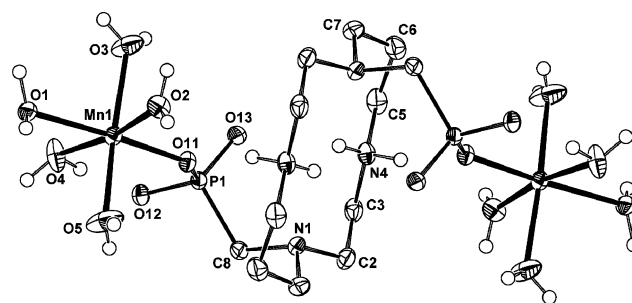


**Fig. 4** Molecular structure of [(H<sub>2</sub>O)<sub>5</sub>Mn<sub>2</sub>(μ-H<sub>2</sub>L)]<sup>2+</sup> cation with atom numbering scheme. Hydrogen atoms attached to carbon atoms are omitted for clarity.

**Table 6** Selected geometric parameters found in the structure of [(H<sub>2</sub>O)<sub>5</sub>Mn<sub>2</sub>(μ-H<sub>2</sub>L)](H<sub>2</sub>L)·21H<sub>2</sub>O

Mn–O11	2.123(2)	O11–Mn–O1	172.05(7)
Mn–O1	2.246(2)	O11–Mn–O2	99.00(7)
Mn–O2	2.146(2)	O11–Mn–O3	88.46(7)
Mn–O3	2.164(2)	O11–Mn–O4A <sup>a</sup>	89.35(8)
Mn–O4A <sup>a</sup>	2.199(3)	O11–Mn–O5	94.83(8)
Mn–O5	2.197(2)	O1–Mn–O2	88.92(7)
		O1–Mn–O3	91.73(7)
P1–O11	1.541(2)	O1–Mn–O4A <sup>a</sup>	82.70(7)
P1–O12	1.533(2)	O1–Mn–O5	86.36(8)
P1–O13	1.519(2)	O2–Mn–O3	83.97(8)
P1–C8	1.826(3)	O2–Mn–O4A <sup>a</sup>	170.06(9)
P2–O21	1.524(2)	O2–Mn–O5	85.77(9)
P2–O22	1.530(2)	O3–Mn–O4A <sup>a</sup>	92.91(10)
P2–O23	1.515(2)	O3–Mn–O5	169.60(10)
P2–C18	1.820(2)	O4A <sup>a</sup> –Mn–O5	98.97(11)

<sup>a</sup> The most abundant position of O4 atom (77%).

The dinuclear complex species lie in the direction of  $z$  axis. The electroneutrality of the crystal is assured by uncoordinated double-deprotonated ligand anion  $(\text{H}_2\text{L})^{2-}$ , which is located in the cavities along  $y$  axis and serves as a counter anion (Fig. S4, ESI†). The skeleton of the anion is severely disordered (Fig. S5, ESI†) and, therefore, correct location of protons on the nitrogen atoms cannot be unambiguously determined; but protonation of secondary amino groups is expected to be analogous to the previous unit and is in accordance with the behaviour of the ligand in solution.<sup>22</sup> The free space in the packing accommodates solvate water molecules. Whole structure is stabilized by an extensive network of medium-to-strong hydrogen bonds between amino groups, coordinated water molecules, phosphonate oxygen atoms and solvate water molecules. Both macrocyclic units (of both coordinated and uncoordinated ligands) are in the same conformation found in most of the structures of cyclam derivatives with diprotonated ring.<sup>4</sup> It should be noted that the  $[\text{Mn}(\text{H}_2\text{O})_5(\text{oxygen donor})]^{2+}$  structure motif in the solid has been observed several times and no structure of manganese(II) complexes with (aminomethyl)phosphonate derivatives contains coordinated nitrogen atom(s) as result of CCDC search.<sup>59</sup> Only the manganese(II) complex of a macrocyclic phosphorus acid derivative is a polymeric  $[\text{Mn}(\text{H}_6\text{dotp})]$  complex ( $\text{H}_8\text{dotp} = 1,4,7,10\text{-tetraazacyclododecane-1,4,7,10-tetrakis(methylphosphonic acid)}$ ) where the pendant arms are bound only through one oxygen atom of a monoprotonated phosphonate moiety and the ring is also protonated on two nitrogen atoms.<sup>60</sup>

#### Kinetics of formation of zinc(II) and cadmium(II) complexes

The formation of zinc(II) and cadmium(II) complexes is relatively slow at pH in the range 3.7–5 which makes it possible to follow the reaction using conventional UV-VIS spectroscopy. As there is no absorbing group or species, indirect indicator method (commonly employed in chemistry of macrocyclic ligands<sup>41,42b,61</sup>) was used to visualize course of the reactions. The method is simple but leads to somewhat less precise results compared with conventional direct methods.<sup>62</sup> At pH higher than 5, the stopped-flow technique was employed as the reactions are noticeably faster.

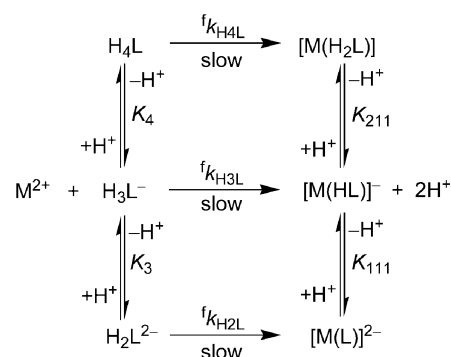
According to the distribution diagram of the free ligand, three differently protonated species,  $\text{H}_4\text{L}$ ,  $\text{H}_3\text{L}^-$  and  $\text{H}_2\text{L}^{2-}$ , are present in an aqueous solution of the ligand in the pH region 3.7–7 (Fig. S6, ESI†). Therefore, each of those ligand species can take part in complexation reaction with  $\text{Zn}^{2+}$  or  $\text{Cd}^{2+}$  ions to form the final  $[\text{M}(\text{H}_n\text{L})]^{n-2}$  ( $n = 0-2$ ) complexes and such particular reactions are characterized by corresponding second-order rate constants  ${}^f k_{\text{H}_n\text{L}}$  ( $n = 2-4$ ) as shown in Scheme 3.

The complex formation from the metal ion and the ligand can be considered as a second-order reaction with the rate law given in eqn (2):

$$v = {}^f k_2 [\text{L}]_{\text{tot}} [\text{M}^{2+}]_{\text{tot}} \quad (2)$$

where  $[\text{L}]_{\text{tot}}$  is total ligand concentration given by eqn (3) considering the ligand protonation constants  $\beta_n$  ( $\beta_n \equiv \beta_{n10}$ ) as defined in the potentiometric section.

$$[\text{L}]_{\text{tot}} = [\text{H}_4\text{L}] + [\text{H}_3\text{L}^-] + [\text{H}_2\text{L}^{2-}] \\ = (\beta_4[\text{H}^+]^4 + \beta_3[\text{H}^+]^3 + \beta_2[\text{H}^+]^2)[\text{L}^{4-}] = a_{\text{L}}[\text{L}^{4-}] \quad (3)$$



**Scheme 3** Formation of 1,8- $\text{H}_4\text{te}2\text{p}$  metal complexes ( $\text{Cu}^{2+}$ ,  $\text{Zn}^{2+}$  and  $\text{Cd}^{2+}$ ).

If the concentration of metal ion is much higher than the concentration of ligand, the eqn (2) could be rewritten into the pseudo-first order rate law given by eqn (4):

$$v = k_{\text{obs}} [\text{L}]_{\text{tot}} \quad (4)$$

where  $k_{\text{obs}}$  is the observed pseudo-first rate constant linearly dependent on the metal ion concentration defined by eqn (5).

$$k_{\text{obs}} = {}^f k_2 [\text{M}^{2+}]_{\text{tot}} \quad (5)$$

The rate law developed from the general Scheme 1 is represented by eqn (6) (as in this case  $[\text{M}^{2+}]_{\text{tot}} = [\text{M}^{2+}]$ ).

$$v = {}^f k_{\text{H}_4\text{L}} [\text{H}_4\text{L}] [\text{M}^{2+}] + {}^f k_{\text{H}_3\text{L}} [\text{H}_3\text{L}^-] [\text{M}^{2+}] + {}^f k_{\text{H}_2\text{L}} [\text{H}_2\text{L}^{2-}] [\text{M}^{2+}] \quad (6)$$

Combining eqns (2), (3) and (6), one obtains eqn (7), which can be simplified to give eqn (8).

$${}^f k_2 a_{\text{L}} [\text{L}^{4-}] [\text{M}^{2+}] = {}^f k_{\text{H}_4\text{L}} \beta_4 [\text{H}^+]^4 [\text{L}^{4-}] [\text{M}^{2+}] \\ + {}^f k_{\text{H}_3\text{L}} \beta_3 [\text{H}^+]^3 [\text{L}^{4-}] [\text{M}^{2+}] + {}^f k_{\text{H}_2\text{L}} \beta_2 [\text{H}^+]^2 [\text{L}^{4-}] [\text{M}^{2+}] \quad (7)$$

$${}^f k_2 a_{\text{L}} = {}^f k_{\text{H}_4\text{L}} \beta_4 [\text{H}^+]^4 + {}^f k_{\text{H}_3\text{L}} \beta_3 [\text{H}^+]^3 + {}^f k_{\text{H}_2\text{L}} \beta_2 [\text{H}^+]^2 \quad (8)$$

Therefore, the dependence of the evaluated second-order rate constant on proton concentration can be expressed by eqn (9).

$${}^f k_2 = \frac{{}^f k_{\text{H}_4\text{L}} \beta_4 [\text{H}^+]^4 + {}^f k_{\text{H}_3\text{L}} \beta_3 [\text{H}^+]^3 + {}^f k_{\text{H}_2\text{L}} \beta_2 [\text{H}^+]^2}{a_{\text{L}}} \quad (9)$$

At the first stage, it was proved that the collected data correspond to a first-order process with respect to the metal ion. It was shown that the dependence of the pseudo-first order rate constant (measured at constant pH) is a linear function of metal ion concentration (according to eqn (5)). Examples of the experimental data and their analysis are available in the ESI.† Therefore, a formation of complexes with higher metal-to-ligand ratio (e.g.  $\text{M}_2\text{L}$ ) can be excluded. In the next step, the obtained second-order formation rate constants  ${}^f k_2$  (see ESI,†) were treated as a function of proton concentration (according to eqn (9)), testing various kinetic models with a set of partial rate constants in order to obtain the best fit for the experimental data.

The dependence given in eqn (9) was used previously for description of kinetics of formation of  $\text{Cu}^{2+}\text{-H}_4\text{L}$  complex.<sup>33</sup> The set of experimental data for copper(II) complexation was extended to the pH region 5.0–7.0 compared with the original paper and re-fitted by eqn (9) with the same results as those reported in the original work.<sup>33</sup> The values of the particular rate constants are listed in Table 7 and the fit is included in Fig. 5. The ligand shows a high kinetic selectivity for complexation of  $\text{Cu}^{2+}$  ion in

**Table 7** Summary of partial rate constants of formation of divalent metal ions complexes with H<sub>4</sub>L (25 °C, 0.1 M KCl)

Rate constant/dm <sup>3</sup> mol <sup>-1</sup> s <sup>-1</sup>	Cu <sup>2+</sup> <sup>a</sup>	Zn <sup>2+</sup>	Cd <sup>2+</sup>
<sup>t</sup> k <sub>H<sub>4</sub>L</sub>	0.17(5)	—	0.15(5)
<sup>t</sup> k <sub>H<sub>3</sub>L</sub>	1.4(2) × 10 <sup>3</sup>	7.4(1)	9.1(4)
<sup>t</sup> k <sub>H<sub>2</sub>L</sub>	2.0(4) × 10 <sup>5</sup>	3.3(3) × 10 <sup>2b</sup>	1.3(2) × 10 <sup>2</sup>
<sup>t</sup> k <sub>OH</sub>	—	1.0 × 10 <sup>5c</sup>	—
<sup>t</sup> k <sub>H<sub>3</sub>L</sub> / <sup>t</sup> k <sub>H<sub>4</sub>L</sub>	8.2(3) × 10 <sup>3</sup>	46 <sup>d</sup>	61(20)
<sup>t</sup> k <sub>H<sub>2</sub>L</sub> / <sup>t</sup> k <sub>H<sub>3</sub>L</sub>	1.4(3) × 10 <sup>2</sup>	44(4)	14(2)

<sup>a</sup> Taken from ref. 33 (25 °C, 0.1 M (K,H)Cl). <sup>b</sup> Value of <sup>t</sup>k<sub>H<sub>3</sub>L</sub> = 1.0 dm<sup>3</sup> mol<sup>-1</sup> s<sup>-1</sup> was reported for formation of Zn<sup>2+</sup>-cyclam complex, ref. 65. <sup>c</sup> Rough estimate. Value of <sup>t</sup>k<sub>OH</sub>/<sup>t</sup>k<sub>H<sub>2</sub>L</sub> ratio is ~300. <sup>d</sup> Estimated values using an average value of <sup>t</sup>k<sub>H<sub>3</sub>L</sub> for Cu<sup>2+</sup> and Cd<sup>2+</sup> ions.

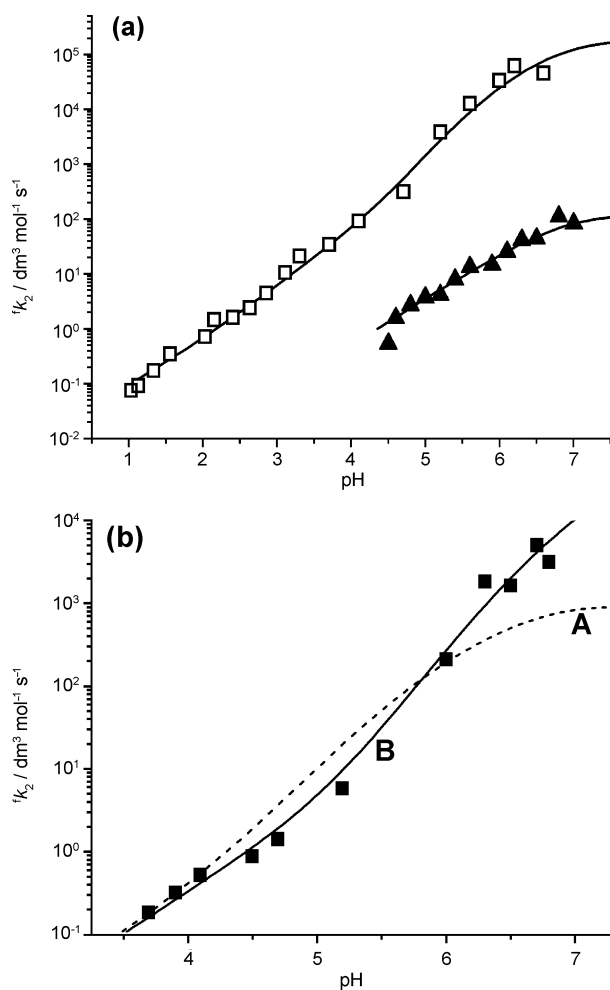
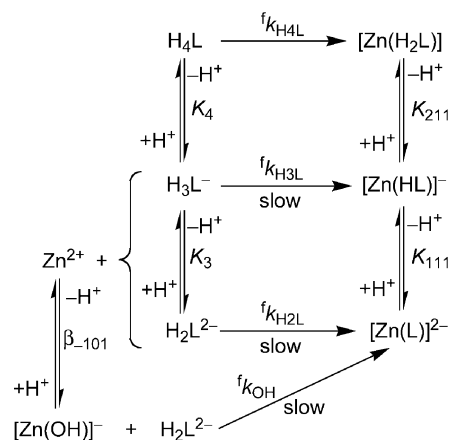


**Fig. 5** The pH dependence of the second-order rate constant <sup>t</sup>k<sub>2</sub> for the formation of complexes of 1,8-H<sub>4</sub>te2p with divalent metal ions. (a) Fitting by eqn (9) (full lines) for Cu<sup>2+</sup> (open squares) and Cd<sup>2+</sup> (full triangles). (b) Fitting by eqn (10) (Zn<sup>2+</sup>, full squares); line A (dashed) represents fitting by model with participation of H<sub>3</sub>L<sup>-</sup> and H<sub>2</sub>L<sup>2-</sup> species only; line B (full) represents the final model with rate constants corresponding to H<sub>3</sub>L<sup>-</sup> and H<sub>2</sub>L<sup>2-</sup> as well as [Zn(OH)]<sup>+</sup> (or HL<sup>3-</sup>) species optimized simultaneously.

acid solutions (pH = 3.7–5.5, Fig. 5) over the other metal ions, and these experimental conditions have been already employed in analytical applications.<sup>34,35</sup> Both other metal ions (Zn<sup>2+</sup>, Cd<sup>2+</sup>) show a very similar reactivity in the pH region 3.7–5.5, but the formation of zinc(II) complexes is noticeably accelerated at higher



**Scheme 4** Formation of zinc(II) complex of 1,8-H<sub>4</sub>te2p.

pH (Fig. 5), where the kinetic selectivity of copper(II) complexation with respect to that of Zn<sup>2+</sup> ion disappears.

In the case of Cd<sup>2+</sup> ion, the experimental data can be sufficiently fitted by eqn (9) affording the values of rate constants for all three expected pathways, similarly as it was observed for copper(II) complexation (Table 7). In the case of zinc(II) complexation, the fit according to eqn (9) is in a good agreement with the experimental data at pH < 5; however, the acceleration at pH > 5.5 cannot be successfully described by eqn (9). Therefore, an additional reaction pathway must be taken into account. The acceleration can be attributed to the reaction of monohydroxo species [Zn(OH)]<sup>+</sup> (more correctly [Zn(H<sub>2</sub>O);(OH)]<sup>+</sup> species) as, in general, hydroxo species are more reactive than aqua ions. The calculated speciation of metal hydroxo complexes in dependence on pH also supports this hypothesis, as [Zn(OH)]<sup>+</sup> is abundant in the pH range 5–6.8 (0.01–0.8%) (Fig. S11, ESI<sup>†</sup>). Furthermore, in the case of the other two metal ions, analogous hydroxo complexes are formed in appreciable abundance at much higher pH (Fig. S11, ESI<sup>†</sup>) and, therefore, their concentration in the pH range used for the complexations is negligible. Therefore, the reactions compiled in Scheme 4 were taken into account for zinc(II) complexation. According to Scheme 4, the dependence of the evaluated second-order rate constant on proton concentration can be derived similarly as in the previous case and is given by eqn (10) where  $a_{Zn} = 1 + \beta_{-101}/[H^+]$ .

$${}^t k_2 = \frac{{}^t k_{H_4L} \beta_4 [H^+]^4 + {}^t k_{H_3L} \beta_3 [H^+]^3 + {}^t k_{H_2L} \beta_2 [H^+]^2 + {}^t k_{OH} \beta_2 \beta_{-101} [H^+]}{a_L a_{Zn}} \quad (10)$$

However, for the zinc(II) system, the value of <sup>t</sup>k<sub>H<sub>4</sub>L</sub> could not be calculated due to numerical difficulties in fitting (the parameter was negative) but it is assumed to be of the same order of magnitude as for copper(II) and cadmium(II). This parameter is not important for the fitting and, therefore, it was not included in the further calculations, but the values of all other rate-constants can be determined from simultaneous fitting and are given in Table 7. The best fit is shown in Fig. 5. On the other hand, the same effect can be ascribed to the acceleration caused by the reaction of the monoprotonated ligand species, which gives the same pH-dependence of the rate constants due to the proton ambiguity. Analogous proton ambiguity and acceleration of complex formation was observed in a study of formation kinetics

of lead(II) with  $N,N',N'',N'''$ -tetrakis(carbamoylmethyl)cyclam derivatives.<sup>63</sup> In our case, we suggest that involvement of the hydroxo species is correct as the effect was observed only for zinc(II) complexation, where the abundance (Fig. S11, ESI†) of hydroxo species is the highest among the studied metal ions. The  $H_2L^{2-}$  species exhibit a very compact solution structure stabilized by intramolecular hydrogen bonds and the structure is similar to that observed for  $H_4L$  in the solid state (Fig. S12, ESI†).<sup>22</sup> The final two dissociation constants of 1,8- $H_4te2p$  are very high (much higher than those for cyclam or  $H_4teta$ ), which leads to an extremely low concentration of monoprotonated species in the pH range employed.<sup>22</sup> In addition, the  $HL^{3-}$  species should have a low abundance even under equilibrium conditions as only one dissociation constant corresponding to last two dissociation steps could be determined.<sup>22</sup> Thus, we believe that pathway involving  $HL^{3-}$  species can be omitted. An acceleration of bound-to-bulk water exchange rates for monohydroxo-aqua complexes in comparison with aqua complexes was observed.<sup>64</sup> A relative acceleration of the pathway involving the  $[Zn(OH)]^+$  and  $H_2L^{2-}$  species conforms to the range of accelerations of solvent exchange observed for the simple hydroxo-aqua species.

Monoprotonated ligand species were used for interpretation of an increased reactivity of several macrocyclic ligands in reactions of  $Zn^{2+}$  ion, such as cyclen ( $k_{HL} = 1.3 \times 10^5 \text{ dm}^3 \text{ mol}^{-1} \text{ s}^{-1}$ ),<sup>65</sup> cyclam ( $k_{HL} = 7.5 \times 10^4$  and  $5.0 \times 10^4 \text{ dm}^3 \text{ mol}^{-1} \text{ s}^{-1}$ )<sup>65,66</sup> or  $H_4dota$  and  $H_4teta$  ( $k_{HL} = 1.1 \times 10^7$  and  $1.6 \times 10^8 \text{ dm}^3 \text{ mol}^{-1} \text{ s}^{-1}$ , respectively).<sup>41</sup> The data for these ligands were determined in a lower-pH region and the mechanism involving hydroxo species was not considered. To compare the rate constants for these ligands, we fitted our experimental data taking into account a rate constant corresponding to the  $HL^{3-}$  species instead of  $k_{OH}$ . The value of such rate constant ( $2.5 \times 10^{10} \text{ dm}^3 \text{ mol}^{-1} \text{ s}^{-1}$ ) is higher than those above.

The highest rate found for the phosphonate ligand is in agreement with a generally accepted model for formation of complexes of polyazamacrocyclic ligands bearing ligating pendant arms.<sup>67–69</sup> In the mechanism, (partially) deprotonated pendant groups are rapidly bound to the metal aqua ion forming an intermediate complex.<sup>42b,61</sup> It is followed by a rate-determining step involving metal ion transfer into the macrocyclic cavity with simultaneous proton(s) removal from the protonated ring nitrogen atom(s) and/or ring conformation rearrangement. Phosphonate moiety exhibits the highest complex-forming ability (combination of its highest basicity and higher overall charge) among the ligands above (no pendant arms for cyclen and cyclam or carboxylate arms for  $H_4dota$  and  $H_4teta$ ). Thus, it forms the most stable intermediate complex, mainly with hard metal ions. In addition, a high hydrogen bond-forming ability of phosphonate groups assists the removal of proton(s) from the macrocyclic cavity.

The formation reactions (characterized by the partial formation constants) for all three metal ions are much slower than water exchange for the corresponding aqua complexes. The highest rate observed for  $Cu^{2+}$  ion compared to the other ions reflects a generally fast ligand exchange observed for the ion due to Jahn–Teller effect and the fastest water exchange rate.<sup>64</sup> As relative differences in the formation rates between the ions are higher than differences in water exchange rate of the aqua ions, a high affinity of  $Cu^{2+}$  ion to nitrogen atoms of the ligand should be taken into account.<sup>44b,61</sup> This ion is probably the most easily transferred

into the macrocyclic cavity in a rate-determining step. Despite a slower water exchange rate on zinc(II) aqua ion compared with cadmium(II) aqua ion, the title ligand reacts more quickly with  $Zn^{2+}$  than  $Cd^{2+}$  ion. If we accept a mechanism assumed for complexation of macrocycles with ligating side chains given above, the difference can be a consequence of a higher stability of a kinetic intermediate (where only phosphonate group(s) are bound) with small and hard  $Zn^{2+}$  ion.

To compare the reactivity of variously protonated species of 1,8- $H_4te2p$ , the ratios of the partial rate constants were calculated (Table 7). In all cases, high values of the  $k_{H_3L}/k_{H_4L}$  and  $k_{H_2L}/k_{H_3L}$  ratios represent the complexation reaction acceleration. It can be caused by differences in charges of the species and/or easier structural rearrangement of less protonated ligand forms.<sup>22</sup> The highest differences in the  $k_{H_3L}/k_{H_4L}$  and  $k_{H_2L}/k_{H_3L}$  ratios for  $Cu^{2+}$  ion are similar to those reported for reactivity of various protonated forms of other cyclam derivatives with the ion.<sup>70</sup>

### Dissociation kinetics of zinc(II) and cadmium(II) complexes

The dissociation kinetics of zinc(II) and cadmium(II) complexes of 1,8- $H_4te2p$  was studied in the pH ranges 3.7–4.8 ( $Zn^{2+}$ ) and 4.5–6.1 ( $Cd^{2+}$ ), where the reactions occur with an optimal rate to be followed by conventional techniques. The dissociation of the zinc(II) complex was followed by UV-VIS spectroscopy using scavengers of either released ligand ( $Cu^{2+}$ ) or  $Zn^{2+}$  (PAR) and the results of both methods are in a satisfactory agreement. This was verified from statistical point of view by analysis of experimental data from pH region 4.12–4.71 where the experimental points show the highest difference. The dissociation of the cadmium(II) complex was determined by the ligand scavenging with  $Cu^{2+}$  ion. The dependences of the pseudo-first-order rate dissociation constants on pH are given in Fig. 6 and the  $k_{obs}$  are given in ESI.†

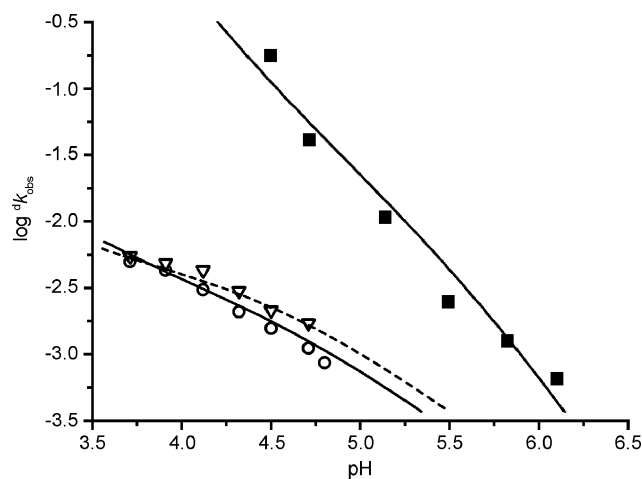
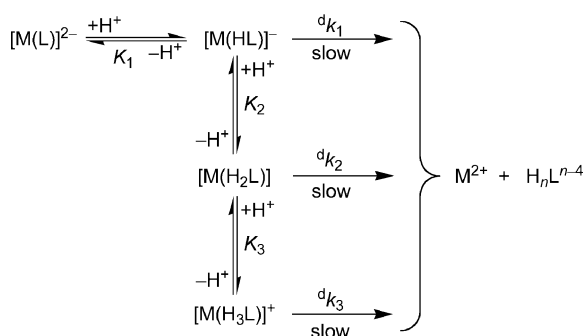


**Fig. 6** The pH dependence of pseudo-first-order rate constants for dissociation of  $[M(L)]^{2-}$  complexes;  $M = Zn^{2+}$  with  $Cu^{2+}$  (open circles, full line) and PAR (open triangles, dashed line) as scavengers,  $M = Cd^{2+}$  with  $Cu^{2+}$  as scavenger (full squares, full line). The experimental points were fitted by eqn (16) only ( $Zn^{2+}$ ) or with the additional term corresponding to  $[Cd(H_4L)]^{2+}$  species ( $Cd^{2+}$ ) with the parameters listed in Table 8.

For fitting of the experimental data, the following mechanism can be suggested (Scheme 5). Here, the constants  $K_1$ – $K_3$



**Scheme 5** The proposed reaction scheme for dissociation of  $[M(L)]^{2-}$  complexes ( $M = \text{Zn}^{2+}, \text{Cd}^{2+}$ ).

correspond to the protonation equilibrium of the complexes given by eqns (11)–(13) (charges are omitted).

$$K_1 = [M(\text{HL})]/[M(L)][\text{H}] \quad (11)$$

$$K_2 = [M(\text{H}_2\text{L})]/[M(\text{HL})][\text{H}] \quad (12)$$

$$K_3 = [M(\text{H}_3\text{L})]/[M(\text{H}_2\text{L})][\text{H}] \quad (13)$$

The rate law for the proposed reaction mechanism is defined in eqn (14).

$$v = {}^d k_{\text{obs}}[\text{complex}]_{\text{tot}} = {}^d k_1[M(\text{HL})] + {}^d k_2[M(\text{H}_2\text{L})] + {}^d k_3[M(\text{H}_3\text{L})] \quad (14)$$

In the given pH regions (3.7–4.8 for zinc(II) complex and 4.5–6.1 for cadmium(II) complex), only  $[M(\text{HL})]^-$  and  $[M(\text{H}_2\text{L})]$  species are present in a high abundance. The amounts of deprotonated complexes is negligible (Fig. 1) and the concentration of the  $[M(\text{H}_3\text{L})]^+$  complex should be also very low as value of  $\log K_3$  for the  $[M(\text{H}_3\text{L})]^+$  species (Scheme 5) is much lower than that of  $\log K_2$  for the  $[M(\text{H}_2\text{L})]$  species (*cf.*  $\log K_3 = 1.21$  and  $1.52$  vs.  $\log K_2 = 5.15$  and  $5.27$  reported for two isomeric  $[\text{Cu}(\text{H}_3\text{L})]^+$  and  $[\text{Cu}(\text{H}_2\text{L})]$  complexes;<sup>33</sup>  $\log K_3 = 1.15$  and  $\log K_2 = 4.78$  for *cis*-O,O- $[\text{Ni}(\text{H}_3\text{L})]^+$  and *cis*-O,O- $[\text{Ni}(\text{H}_2\text{L})]$  complexes<sup>31</sup>). Therefore, eqn (15) can be postulated.

$$v = {}^d k_{\text{obs}}[\text{complex}]_{\text{tot}} = {}^d k_{\text{obs}}([M(\text{HL})] + [M(\text{H}_2\text{L})]) \quad (15)$$

By rearrangement of eqns (11)–(15), the final rate law can be obtained (eqn (16)).

$${}^d k_{\text{obs}} = \frac{k_1 + {}^d k_2 K_2 [\text{H}^+] + {}^d k_3 K_2 K_3 [\text{H}^+]^2}{1 + K_2 [\text{H}^+]} \quad (16)$$

Eqn (16) formally corresponds to the equation used for fitting of acid-assisted dissociation data for the *pc*- $[\text{Cu}(\text{H}_4\text{L})]^{2+}$  complex.<sup>33</sup> An analogous rate law has been described recently for dissociation of the lead(II) complex of *N,N',N'',N'''*-tetrakis(carbamoylmethyl)cyclam.<sup>63</sup>

The pseudo-first-order rate constants,  ${}^d k_{\text{obs}}$ , for both divalent metal complexes were fitted through the experimental points by the eqn (16). The values of protonation constants,  $\log K_2 = 4.44$  for zinc(II) and  $\log K_2 = 5.59$ , for cadmium(II) complexes, respectively, were taken from Table 2. The best fits of experimental data are shown in Fig. 6 and the resulting values in Table 8.

The dissociation pathways with participation of the  $[M(\text{HL})]^-$  complex species were not observed ( ${}^d k_1 = 0$ ). In the case of the zinc(II) complex, two reaction pathways of complex dissociation with two respective rate constants (for the  $[\text{Zn}(\text{H}_2\text{L})]$  and  $[\text{Zn}(\text{H}_3\text{L})]^+$  species) were resolved (Scheme 5). On the contrary, in the case of the cadmium(II) complex, the reaction pathways through triprotonated and, possibly, tetraprotonated species were identified, probably due to a very slow dissociation of the diprotonated species as only the upper limit of the corresponding rate constant  ${}^d k_2$  could be estimated (Table 8). Involving a term corresponding to dissociation of the  $[\text{Cd}(\text{H}_4\text{L})]^{2+}$  species ( ${}^d k_4 K_4 K_3 [\text{H}^+]^3$ ) into eqn (16) led to a slight improvement of the fitting in the most acid region; the inclusion of this term did not change values in Table 8. However, only very rough estimate  ${}^d k_4 K_4 K_3 \approx 5 \times 10^7$  ( $\text{dm}^3 \text{mol}^{-1}$ )<sup>2</sup>  $\text{s}^{-1}$  could be obtained for the  $[\text{Cd}(\text{H}_4\text{L})]^{2+}$  pathway. Comparing the dissociation rate constants of both metal complexes, decomposition reaction pathways involving the triprotonated species are much more important than other reaction steps involving the less ( $[M(\text{H}_2\text{L})]$ ) or, possibly, more protonated ( $[\text{Cd}(\text{H}_4\text{L})]^{2+}$ ) species under experimental conditions used in the study. This phenomenon can be demonstrated by the calculated ratio of the rate constants ( ${}^d k_3 K_3$ )/ ${}^d k_2$  for both pathways for the zinc(II) complex ( $1.9 \times 10^3$ ) while this ratio is even higher by several orders of magnitude for the cadmium(II) complex. It can be assumed that both  $[M(\text{H}_2\text{L})]$  species are hardly protonated and corresponding protonation constant of the  $[M(\text{H}_2\text{L})]$  species should be in range of  $\log K_3 = 1$ – $2$ . Therefore, the concentration of the triprotonated reaction intermediates is on a trace level under the experimental conditions used in this study. Their high reactivity is probably caused by the fact that the third proton can be very easily transferred to a nitrogen atom leading to fast decomposition of such complex species. The overall inertness of the complexes decreases in the order  $\text{Cu}(\text{II}) \gg \text{Zn}(\text{II}) > \text{Cd}(\text{II})$ . This trend is related to the metal ion size (fitting the macrocyclic cavity) and

**Table 8** Summary of partial dissociation rate constants determined (eqn 16) for acid-assisted hydrolysis of  $[M(L)]^{2-}$  complexes ( $M = \text{Zn}^{2+}, \text{Cd}^{2+}$ ) (25 °C, 0.1 M KCl)

Rate constant	$\text{Cu}^{2+}$ <sup>a</sup>	$\text{Zn}^{2+}$		
		PAR scavenger	$\text{Cu}^{2+}$ scavenger	$\text{Cd}^{2+}$
${}^d k_2/\text{s}^{-1}$	$8.5(3) \times 10^{-4}$	$4.6(5) \times 10^{-3}$	$3.2(1) \times 10^{-3}$	$<3 \times 10^{-4b}$
${}^d k_3 K_3/\text{dm}^3 \text{mol}^{-1} \text{s}^{-1}$	$9.7(1.2) \times 10^{-5}$	$8.9(1.3)$	$17.6(1.2)$	$2.48(6) \times 10^3$
$({}^d k_3 K_3/{}^d k_2)/\text{dm}^3 \text{mol}^{-1}$	0.114(6)	$1.9(3) \times 10^3$	$5.5(4) \times 10^3$	$>10^7$

<sup>a</sup> Reported<sup>33</sup> for *pc*- $[\text{Cu}(\text{H}_4\text{L})]^{2+}$  complex species,  $t = 25.0$  °C,  $I = 5.0$  M (Na,H)ClO<sub>4</sub>. <sup>b</sup> Only an upper estimate.

their affinity to nitrogen or oxygen atoms (strength of the  $M^{2+}-N$  and  $M^{2+}-O$  bonds).

## Conclusions

We have studied interactions of divalent metal ions with a bis(methylphosphonate) cyclam derivative. In the solid state, the structures of the complexes clearly depend on the relative affinity of the central ion to different donor atoms of the ligand. The diprotonated zinc(II) complex is mononuclear with all available donor atoms coordinated. In both diprotonated manganese(II) and lead(II) complexes, the central metal ion binds only oxygen donors and nitrogen atoms are unbound and protonated. The determination of stability constants reveals a high preference of complexation of transition-metal ions, and in particular a high selectivity to the  $Cu^{2+}$  ion. In the complexes with transition metals, the nitrogen atoms of the macrocycle are coordinated to the metal ion from the beginning of the complexation in acid solutions. The ligand has a low affinity to alkaline earth ions, and the nitrogen atoms are coordinated to the central metal ions only in strongly alkaline solutions, similarly as it was found for other cyclam derivatives. The behaviour of lead(II) and manganese(II) complexes is somewhere in between the previous groups, with deprotonation of the amino groups induced by metal in slightly alkaline region. The kinetics of formation of zinc(II) and cadmium(II) complexes follows the common mechanism assumed for complex formation of macrocycles bearing coordinating pendant arms. It shows a high difference in reactivity between differently protonated ligand species. Complexes of  $Zn^{2+}$  and  $Cd^{2+}$  ions are rather unstable in acid-assisted decomplexation in comparison with the corresponding copper(II) and nickel(II) complexes. The zinc(II) complex is much more kinetically inert than the cadmium(II) complex (Fig. 6). This inertness is associated with the suitability of the size and conformation of the macrocycle cavity. The smaller metal ions such as  $Cu^{2+}$  or  $Zn^{2+}$  fit the cavity better than the larger ones as  $Cd^{2+}$  ion. The results confirm that 1,8- $H_4te2p$  is a very suitable ligand for selective binding of divalent copper, e.g. in nuclear medicine applications.

## Acknowledgements

We thank Dr K. Lang (Institute of Inorganic Chemistry, Academy of Sciences of the Czech Republic) for the use of stopped-flow apparatus and Dr I. Císařová for X-ray data acquisition. This work was supported by the Grant Agency of the Czech Republic (No. 203/06/0467) and EU FP6 Network of Excellence EMIL (No. LSHC-2004-503569) and DiMI (No. LSHB-2005-512146) projects.

## References

- 1 A. E. Martell and R. D. Hancock, *Metal Complexes in Aqueous Solutions*, Plenum Press, New York, 1996.
- 2 S. F. Lincoln, *Coord. Chem. Rev.*, 1997, **166**, 255.
- 3 K. P. Wainwright, *Coord. Chem. Rev.*, 1997, **166**, 35.
- 4 M. Meyer, V. Dahaoui-Ginderrey, C. Lecomte and R. Guilard, *Coord. Chem. Rev.*, 1998, **178–180**, 1313.
- 5 L. F. Lindoy, *Adv. Inorg. Chem.*, 1998, **45**, 75.
- 6 S. Aime, M. Botta, M. Fasano and E. Terreno, *Acc. Chem. Res.*, 1999, **32**, 941.
- 7 P. Caravan, J. J. Ellison, T. J. Mc Murry and R. B. Laufer, *Chem. Rev.*, 1999, **99**, 2293.
- 8 A. E. Merbach and É. Tóth, *The Chemistry of Contrast Agents in Medical Magnetic Resonance Imaging*, Wiley, Chichester, UK, 2001.
- 9 *Topics in Current Chemistry*, Springer, Heidelberg, Germany, 2002, vol. 221.
- 10 C. J. Anderson and M. J. Welch, *Chem. Rev.*, 1999, **99**, 2219.
- 11 W. A. Volkert and T. J. Hoffmann, *Chem. Rev.*, 1999, **99**, 2269.
- 12 (a) S. Liu, *Chem. Soc. Rev.*, 2004, **33**, 445; (b) S. Liu and D. S. Edwards, *Bioconjugate Chem.*, 2001, **12**, 7.
- 13 *Handbook of Radiopharmaceuticals. Radiochemistry and Applications*, ed. M. J. Welch and C. S. Redvanly, Wiley, Chichester, UK, 2003.
- 14 W. P. Li, L. A. Meyer and C. J. Anderson, *Top. Curr. Chem.*, 2005, **252**, 179.
- 15 D. Parker, R. S. Dickins, H. Puschmann, C. Crossland and J. A. K. Howard, *Chem. Rev.*, 2002, **102**, 1977.
- 16 S. Faulkner and J. L. Matthews, in *Comprehensive Coordination Chemistry II*, ed. J. A. McCleverty and T. J. Meyer, Elsevier, 2004, vol. 9, pp. 913–944.
- 17 S. V. Smith, *J. Inorg. Biochem.*, 2004, **98**, 1874.
- 18 S. Hassfjell and M. W. Brechbiel, *Chem. Rev.*, 2001, **101**, 2019.
- 19 I. Belskii, Y. M. Polikarpov and M. I. Kabachnik, *Usp. Khim.*, 1992, **61**, 415, and references therein.
- 20 A. D. Sherry, *J. Alloys Compd.*, 1997, **249**, 153.
- 21 I. Lukeš, J. Kotek, P. Vojtíšek and P. Hermann, *Coord. Chem. Rev.*, 2001, **216–217**, 287, and references therein.
- 22 J. Kotek, P. Vojtíšek, I. Císařová, P. Hermann, P. Jurečka, J. Rohovec and I. Lukeš, *Collect. Czech. Chem. Commun.*, 2000, **65**, 1289.
- 23 A. D. Sherry, J. Ren, J. Huskens, E. Brücher, E. Tóth, C. F. C. G. Geraldes, M. M. C. A. Castro and W. P. Cacheris, *Inorg. Chem.*, 1996, **35**, 4604.
- 24 X. Sun, M. Wuest, Z. Kovacs, A. D. Sherry, R. Motekaitis, Z. Wang, A. E. Martell, M. J. Welch and C. J. Anderson, *J. Biol. Inorg. Chem.*, 2003, **8**, 217.
- 25 (a) K. Popov, H. Ronkkomaki and L. H. J. Lajunen, *Pure Appl. Chem.*, 2001, **73**, 1641; (b) K. Popov, E. Niskanen, H. Rönkkömäki and L. H. J. Lajunen, *New J. Chem.*, 1999, **23**, 1209.
- 26 (a) F. Marques, L. Gano, M. P. Campello, S. Lacerda, I. Santos, L. M. P. Lima, J. Costa, P. Antunes and R. Delgado, *J. Inorg. Biochem.*, 2006, **100**, 270; (b) K. P. Guerra, R. Delgado, L. M. P. Lima, M. G. B. Drew and V. Félix, *Dalton Trans.*, 2004, 1812; (c) F. Marques, K. P. Guerra, L. Gano, J. Costa, M. P. Campello, L. M. P. Lima, R. Delgado and I. Santos, *J. Biol. Inorg. Chem.*, 2004, **9**, 859; (d) R. Delgado, L. C. Siegfried and T. A. Kaden, *Helv. Chim. Acta*, 1990, **73**, 140.
- 27 I. Lázár, A. D. Sherry, R. Ramasamy, E. Brücher and R. Király, *Inorg. Chem.*, 1991, **30**, 5016.
- 28 K. Bazakas and I. Lukeš, *J. Chem. Soc., Dalton Trans.*, 1995, 1133.
- 29 (a) P. Lubal, M. Kývala, P. Hermann, J. Holubová, J. Rohovec, J. Havel and I. Lukeš, *Polyhedron*, 2001, **20**, 47; (b) J. Rohovec, M. Kývala, P. Vojtíšek, P. Hermann and I. Lukeš, *Eur. J. Inorg. Chem.*, 2000, 195.
- 30 M. Helps, D. Parker, J. R. Murphy and J. Chapman, *Tetrahedron Lett.*, 1989, **45**, 219.
- 31 J. Kotek, P. Vojtíšek, I. Císařová, P. Herman and I. Lukeš, *Collect. Czech. Chem. Commun.*, 2001, **66**, 363.
- 32 J. Kotek, I. Císařová, P. Hermann, I. Lukeš and J. Rohovec, *Inorg. Chim. Acta*, 2001, **317**, 324.
- 33 J. Kotek, P. Lubal, P. Hermann, I. Císařová, I. Lukeš, T. Godula, I. Svobodová, P. Táborský and J. Havel, *Chem. Eur. J.*, 2003, **9**, 233.
- 34 I. Svobodová, P. Lubal, P. Hermann, J. Kotek and J. Havel, *J. Inclusion Phenom. Macrocycl. Chem.*, 2004, **49**, 11.
- 35 I. Svobodová, P. Lubal, P. Hermann, J. Kotek and J. Havel, *Microchim. Acta*, 2004, **148**, 21.
- 36 (a) R. Přibil, *Analytical Applications of EDTA and Related Compounds*, Pergamon Press, Oxford, 1972; (b) G. Schwarzenbach and H. Flaschka, *Complexometric Titrations*, Methuen, London, 1969.
- 37 (a) M. Kývala and I. Lukeš, *Chemometrics'95*, Abstract book p. 63, Pardubice, Czech Republic, 1995; full version of *OPIUM software package* is available (free of charge) on <http://www.natur.cuni.cz/~kyvala/opium.html>; (b) M. Kývala, P. Lubal and I. Lukeš, *IX. Spanish–Italian, and Mediterranean Congress on Thermodynamics of Metal Complexes (SIMEC 98)*, Girona, Spain, 1998.
- 38 (a) A. E. Martell and R. M. Smith, *Critical Stability Constants*, Plenum Press, New York, 1974–1989, vol. 1–6; (b) *NIST Standard*

- 39 C. F. Baes, Jr. and R. E. Mesmer, *The Hydrolysis of Cations*, Wiley, New York, 1976.
- 40 Y. Zhang and M. Muhammed, *Hydrometallurgy*, 2001, **60**, 215.
- 41 S. P. Kasprzyk and R. G. Wilkins, *Inorg. Chem.*, 1982, **21**, 3349.
- 42 (a) E. Balogh, R. Tripier, R. Ruloff and É. Tóth, *Dalton Trans.*, 2005, 1058; (b) K.-Y. Choi, D. W. Kim, C. S. Kim, C. P. Hong, H. Ryu and Y.-I. Lee, *Talanta*, 1997, **44**, 527; (c) É. Tóth, E. Brücher, I. Lázár and I. Tóth, *Inorg. Chem.*, 1994, **33**, 4070; (d) K.-Y. Choi, J. C. Kim and D. W. Kim, *J. Coord. Chem.*, 1993, **30**, 1.
- 43 E. J. Billo, *Excel for Chemists*, Wiley-VCH, New York, 2001.
- 44 Z. Otwinowski and W. Minor, *HKL Denzo and Scalepack Program Package by Nonius BV*, Delft, 1997; Z. Otwinowski and W. Minor, *Methods Enzymol.*, 1997, **276**, 307.
- 45 A. Altomare, M. C. Burla, M. Camalli, G. L. Casciarano, C. Giacovazzo, A. Guagliardi, A. G. G. Moliterni, G. Polidori and R. Spagna, *J. Appl. Crystallogr.*, 1999, **32**, 115.
- 46 G. M. Sheldrick, *SHELXL97. Program for Crystal Structure Refinement from Diffraction Data*, University of Gottingen, Gottingen, 1997.
- 47 X. Liang and P. J. Sadler, *Chem. Soc. Rev.*, 2004, **33**, 246.
- 48 M. K. Moi, C. F. Meares, M. J. McCall, W. C. Cole and S. J. DeNardo, *Anal. Biochem.*, 1985, **148**, 249.
- 49 S. Füzzerová, J. Kotek, I. Císařová, P. Hermann, K. Binnemans and I. Lukeš, *Dalton Trans.*, 2005, 2908.
- 50 S. A. Pisareva, F. I. Belskii, T. Ya. Medved and M. I. Kabachnik, *Izv. Akad. Nauk SSSR, Ser. Khim.*, 1987, 413.
- 51 G. Anderegg, F. Arnaud-Neu, R. Delgado, J. Felcman and K. Popov, *Pure Appl. Chem.*, 2005, **77**, 1445.
- 52 (a) S. Chaves, R. Delgado and J. J. R. Frausto Da Silva, *Talanta*, 1992, **39**, 249; (b) R. Delgado and J. J. R. Frausto Da Silva, *Talanta*, 1982, **29**, 815.
- 53 (a) F. Marques, L. Gano, M. P. Campello, S. Lacerda, I. Santos, L. M. P. Lima, J. Costa, P. Antunes and R. Delgado, *J. Inorg. Biochem.*, 2006, **100**, 270; (b) R. Delgado, J. Costa, K. P. Guerra and L. M. P. Lima, *Pure Appl. Chem.*, 2005, **77**, 569.
- 54 X. Liang, M. Weishäupl, J. A. Parkinson, S. Parsons, P. A. McGregor and P. J. Sadler, *Chem. Eur. J.*, 2003, **9**, 4709.
- 55 B. Bosnich, C. K. Poon and M. Tobe, *Inorg. Chem.*, 1965, **4**, 1102.
- 56 A. Riesen, M. Zehnder and T. A. Kaden, *Acta Crystallogr., Sect. C*, 1991, **47**, 531.
- 57 (a) B.-P. Yang, Z.-M. Sun and J.-G. Mao, *Inorg. Chim. Acta*, 2004, **357**, 1583; (b) J.-L. Song, J.-G. Mao, Y.-Q. Sun, H.-Y. Zeng, R. K. Kremer and A. Clearfield, *J. Solid State Chem.*, 2004, **177**, 633; (c) C. Lei, J.-G. Mao and Y.-Q. Sun, *J. Solid State Chem.*, 2004, **177**, 2449; (d) Z.-M. Sun, J.-G. Mao, B.-P. Yang and S.-M. Ying, *Solid State Sci.*, 2004, **6**, 295; (e) J.-G. Mao, Z. Wang and A. Clearfield, *J. Chem. Soc., Dalton Trans.*, 2002, 4541.
- 58 S.-M. Ying, J.-G. Mao, B. P. Yang and Z.-M. Sun, *Inorg. Chem. Commun.*, 2003, **6**, 1319.
- 59 (a) F. H. Allen, *Acta Crystallogr., Sect. B*, 2002, **58**, 380; (b) A. G. Orpen, *Acta Crystallogr., Sect. B*, 2002, **58**, 398.
- 60 D. Kong, D. G. Medvedev and A. Clearfield, *Inorg. Chem.*, 2004, **43**, 7308.
- 61 K.-Y. Choi, *Polyhedron*, 1997, **16**, 2073.
- 62 R. G. Wilkins, *Kinetics and Mechanism of Reactions of Transition Metal Complexes*, VCH, Weinheim, 1991.
- 63 F. Cuenot, M. Meyer, E. Espinosa and R. Guilard, *Inorg. Chem.*, 2005, **44**, 7895.
- 64 D. T. Richens, *Chem. Rev.*, 2005, **105**, 1961.
- 65 M. Kodama and E. Kimura, *J. Chem. Soc., Dalton Trans.*, 1977, 2269.
- 66 P. Leugger, L. Hertli and T. A. Kaden, *Helv. Chim. Acta*, 1978, **61**, 2296.
- 67 E. Brücher, *Top. Curr. Chem.*, 2002, **221**, 123.
- 68 M. Soibinet, D. Gusmeroli, L. Siegfried, T. A. Kaden, C. Palivan and A. Schweiger, *Dalton Trans.*, 2005, 2138.
- 69 J. Moreau, E. Guillon, J.-C. Pierrard, J. Rimbault, M. Port and M. Aplincourt, *Chem. Eur. J.*, 2004, **10**, 5218.
- 70 P. G. Lye, G. A. Lawrance and M. Maeder, *J. Chem. Soc., Dalton Trans.*, 2001, 2376.